Upconverting nanovesicles for the activation of ruthenium anti-cancer prodrugs with red light

Askes, S.H.C.

CHAPTER 8

Activation of liposome-bound Ru(II) prodrugs using red-to-blue triplet-triplet annihilation upconversion in a biological context

Light upconversion by means of triplet-triplet annihilation upconversion (TTA-UC) is a promising photochemical approach to shift the activation wavelength of photodissociative ruthenium(II) prodrugs to the phototherapeutic window. In this chapter, the biological application of liposomes doped with red-to-blue upconverting TTA-UC dyes and blue-light responsive Ru-prodrugs is addressed. The oxygen-sensitivity of TTA-UC in liposomes was effectively reduced by the addition of water-soluble and biocompatible anti-oxidants. This strategy also resulted in greatly enhanced upconversion emission in living cells. To demonstrate the *in vivo* applicability of upconversion mediated Ru-prodrug release, it was shown that red-to-blue TTA-UC could be generated at a depth of 12 mm in chicken and pork fillet, and that Ru prodrugs could be activated by red-to-blue TTA-UC at a depth of 7 mm in pork fillet under irradiation of a medical grade 630 nm PDT laser. Finally, the photocytotoxicity of the liposomes in combination with red light irradiation was investigated in A549, MCF7, and MRC5 cells. Unfortunately, neither irradiation of Ru-bound prodrugs with blue light (direct activation) nor with red light (mediated by TTA-UC) resulted in high toxicity compared to experiments conducted in the dark, due to the poor overall toxicity of the here-studied Ru complexes. Altogether, the results presented in this chapter provide valuable insights in which requirements need to be fulfilled in the future to achieve photoactivation of Ru-complexes by TTA-UC *in vitro.*

Sven H. C. Askes, Michael S. Meijer, Lucien N. Lameijer, Wim Pomp, Samantha L. Hopkins, Marlize van Breugel, Iris Landman, Tessel Bouwens, Thomas Schmidt, and Sylvestre Bonnet.

8.1 Introduction

Light-activatable ruthenium polypyridyl complexes have received considerable attention as promising anticancer pro-drugs in photoactivated chemotherapy (PACT).[1] It is proposed that upon excitation with visible light, they are transformed from the non-toxic "caged" compound to the cytotoxic species. With such compounds, undesired side-effects for patients can be greatly reduced by the excellent spatio-temporal control over activation. Also, the toxicity does not depend on the presence of oxygen, as opposed to photodynamic therapy (PDT) that functions by generating highly reactive oxygen species (ROS). Thus, using light-activatable Ru-complexes may be suitable for hypoxic tumor tissues for which PDT is not effective. Furthermore, non-covalent binding of ruthenium polypyridyl complexes to PEGylated liposomes by means of a lipophilic anchor-ligand may help targeting these compounds towards tumor tissues by making use of the leaky vasculature of tumors, i.e. the enhanced permeability and retention effect .[2]

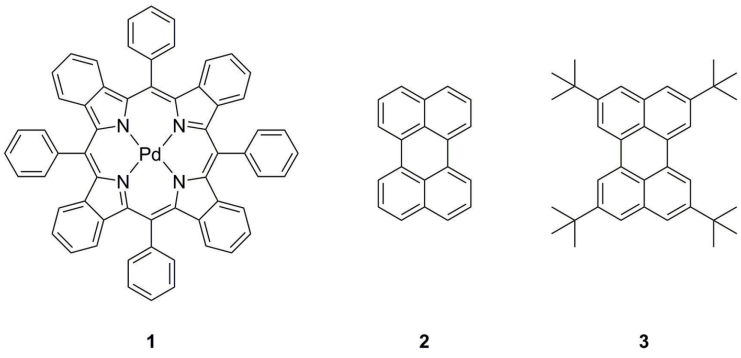

*Figure 8.1. Chemical structures of palladium(II) tetraphenyltetrabenzoporphyrin (**1**), perylene (**2**), and 2,5,8,11-tetra(tert-butyl)perylene (**3**).*

However, most Ru-complexes are only activatable with blue or green light, while those wavelengths do not penetrate human tissue very well. Shifting the excitation wavelength of ruthenium complexes to the phototherapeutic window (600 – 950 nm) by molecular design remains very challenging.[3] To circumvent this problem, upconversion of light can be used to locally "upgrade" red to near-infrared photons to blue or green photons, with which the pro-drug can be activated. Especially the combination of red-to-blue triplet-triplet annihilation upconversion (TTA-UC) and light-sensitive ruthenium complexes on liposomal drug carriers is very promising, as demonstrated in Chapter 3 and Chapter 4.[4] A red-to-blue TTA-UC dye couple

consisting of palladium(II) tetraphenyltetrabenzoporphyrin (**1**) and perylene (**2**, see Figure 8.1) was doped in PEGylated liposomes and used for effectively triggering the photodissociation reaction of [Ru(tpy)(bpy)(thioether-cholesterol)]$^{2+}$ ($\mathbf{4}^{2+}$, see Figure 8.2) to [Ru(tpy)(bpy)(H_2O)]$^{2+}$ ($\mathbf{8}^{2+}$). In further experiments (Chapter 4), lifetime and steady-state spectroscopy experiments revealed that the upconverted blue light of **2** was transferred with ~90% efficiency to $\mathbf{4}^{2+}$ via a Förster resonance energy-transfer (FRET) mechanism when all three molecules were doped in the same liposome membrane.

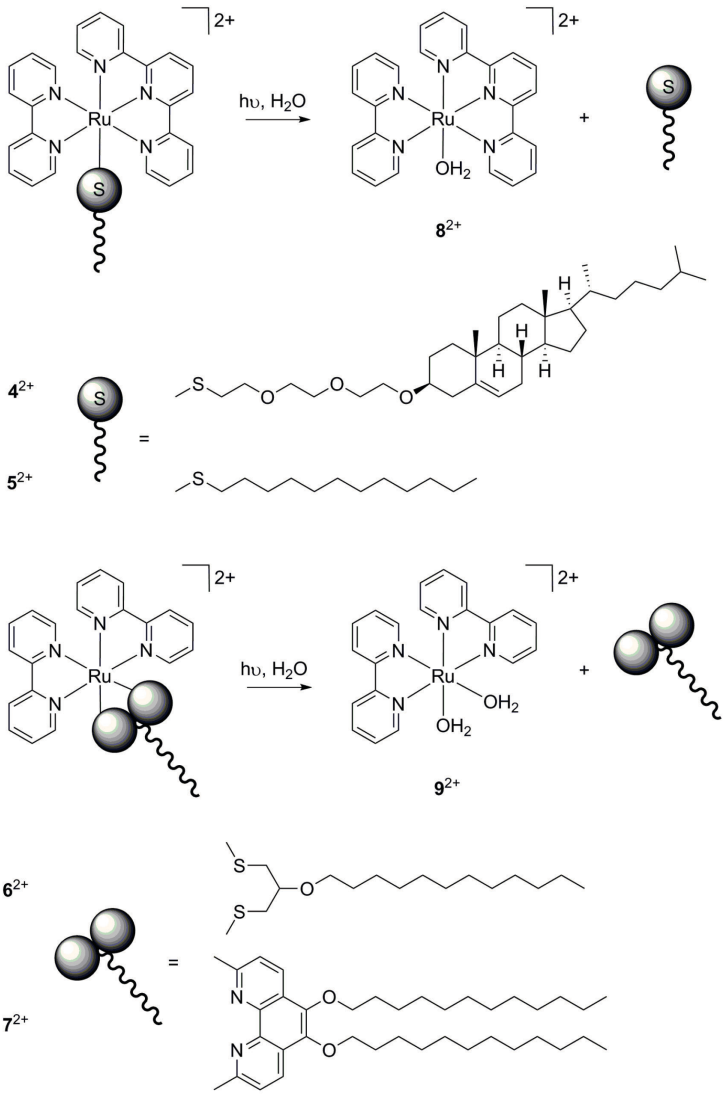

Figure 8.2. Chemical structures of ruthenium polypyridyl complexes $\mathbf{4}^{2+}$, $\mathbf{5}^{2+}$, $\mathbf{6}^{2+}$, and $\mathbf{7}^{2+}$ and their photochemical reaction to the aquated species $\mathbf{8}^{2+}$ or $\mathbf{9}^{2+}$.

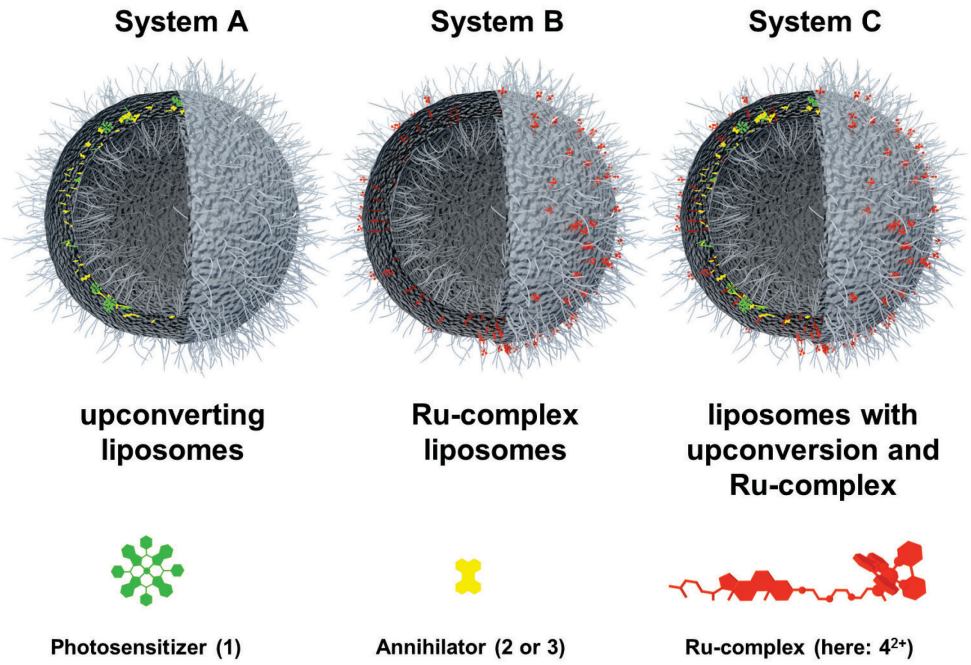

Figure 8.3. Schematic representation of the three liposome systems (System A, B, and C) studied in this chapter. Compound $\mathbf{4}^{2+}$ *features as an example of a Ru-complex which can be anchored to liposome membrane.*

However, the biological application of these upconverting liposomes doped with Ru-prodrugs is not straightforward. Especially the biocompatibility and toxicity of the system, the oxygen sensitivity of the TTA-UC mechanism, and the photoactivation with red light in biological systems have not been addressed so far. Moreover, the (photo)cytotoxicity of Ru-prodrug doped liposomes with blue light irradiation (*i.e.* without upconversion) has not yet been investigated as well. In this chapter, three major types of liposomes will be prepared, called System A, B, and C (Figure 8.3), and their photochemical properties and (photo)cytotoxicity will be evaluated. System A consists of liposomes doped with upconverting dyes **1** and **2** or **1** and **3**; System B consists of liposomes doped with only Ru-complex $\mathbf{4}^{2+}$, $\mathbf{5}^{2+}$, $\mathbf{6}^{2+}$, or $\mathbf{7}^{2+}$; System C consists of liposomes doped with upconverting dyes **1** and **3** and Ru-complex $\mathbf{6}^{2+}$. The following research questions will be addressed:

i. Are red-to-blue upconverting liposomes able to produce upconversion *in vitro* and can the oxygen sensitivity of TTA-UC in cells be reduced? (System A)

ii. Are upconverting liposomes cytotoxic in the dark and what becomes their cytotoxicity under red-light irradiation? (System A)
iii. How are upconverting liposomes digested after uptake? (System A)
iv. Up to which depth can TTA-UC with red-to-blue upconverting liposomes be generated in a model of healthy human tissue? (System A)
v. Is it really advantageous to use red light instead of blue light? Does the greater penetration depth of red light with respect to blue light result in a greater degree of prodrug activation? (System C)
vi. Are liposomes doped with ruthenium complexes (photo)cytotoxic under dark and blue light irradiated conditions? (System B)
vii. Can ruthenium prodrugs on liposomes be activated by red-to-blue TTA-UC *in vitro* in hypoxic conditions? (System C)

8.2 Results and discussion

8.2.1 Liposome preparation

Neutral PEGylated liposomes were prepared by a standard hydration-extrusion protocol in phosphate buffered saline (PBS) as described before (Chapter 3 – Chapter 7). Where applicable, before addition to the lipid film, PBS was supplemented with a known concentration of L-ascorbic acid (L-Asc) and/or glutathione (GSH), and neutralized to *pH* 7.0 – 7.6 with NaOH. The major component of all liposomes was a neutral phospholipid, *i.e.* either 1,2-dilauroyl-*sn*-glycero-3-phosphocholine (DLPC, liposomes denoted with L in Table 8.1) or 1,2-dimyristoyl-*sn*-glycero-3-phosphocholine was used (DMPC, liposomes denoted with M). The liposomes were PEGylated with 4 mol% sodium N-(carbonyl-methoxy polyethyleneglycol-2000)-1,2-distearoyl-*sn*-glycero-3-phospho ethanolamine (DSPE-mPEG-2000), which is known to prevent aggregation and prolong the blood-circulation lifetime of liposomes.[2] Finally, the liposomes were doped with either the TTA-UC dye couple (System A; 0.05 mol% **1**, 0.5 mol% **2** or **3**), or Ru-complex (System B; 4 mol% $\mathbf{4}^{2+}$, $\mathbf{5}^{2+}$, $\mathbf{6}^{2+}$, or $\mathbf{7}^{2+}$), or all three components (System C; 0.05 mol% **1**, 1 mol% **3**, and 4 mol% $\mathbf{6}^{2+}$); see Figure 8.3 for a schematic representation of systems A, B, and C and Table 8.1 for the exact liposome formulations and the codes used to name all liposomes. Incorporation of all dopants in the final samples was complete, as the extrusion filter during liposome preparation remained almost colorless. Dynamic light scattering (DLS) experiments revealed that the

hydrodynamic size (z-ave) of all liposomes varied from 130 – 170 nm with an average polydispersity index (PDI) of 0.1.

Table 8.1. Summary of liposome formulations used in this chapter. Liposomes with designation L or M are made with DLPC or DMPC as main lipid, respectively.

System	Code	[DMPC] mM	[DLPC] mM	[PEG][a] mM	[**1**] µM	[**2**] µM	[**3**] µM	[$\mathbf{4}^{2+}$] µM	[$\mathbf{5}^{2+}$] µM	[$\mathbf{6}^{2+}$] µM	[$\mathbf{7}^{2+}$] µM
A	**L1-2**		5.0	0.20	2.5	25					
	M1	5.0		0.20	2.5						
	M2	5.0		0.20		25					
	M3	5.0		0.20			25				
	M1-3	5.0		0.20	2.5		25				
B	**M4**	5.0		0.20				200			
	M5	5.0		0.20					200		
	M6	5.0		0.20						200	
	M7	5.0		0.20							200
C	**L1-3-6**		5.0	0.20	2.5		50			200	
	M1-3-6	5.0		0.20	2.5		50			200	
	M3-6	5.0		0.20			50			200	

[a] PEG = DSPE-mPEG-2000

8.2.2 Anti-oxidants protect TTA-UC in DLPC liposomes in air in solution

One strategy of reducing the oxygen-sensitivity of TTA-UC in liposomes is the addition of water soluble anti-oxidants that react with ground state or singlet state oxygen to chemically deoxygenate the solution. To evaluate the influence of water-soluble anti-oxidants on TTA-UC, red-to-blue upconverting PEGylated DLPC liposomes (**L1-2**) were mixed with various amounts of L-Asc or GSH. Here, DLPC was used as main lipid, because red-to-blue TTA-UC was found to be much more efficient at room temperature in DLPC than DMPC liposomes (Chapter 6). The UV-vis absorbance spectrum of **L1-2** in presence of 5 mM L-Asc shows the typical absorption peaks of **2** between 375 and 450 nm, and the absorption peaks of **1** at 440 and 630 nm (Figure 8.4a). A small band below 400 nm was attributed to absorption of L-Asc and oxidized ascorbate products. When the sample was irradiated with 10 mW 630 nm light (80 mW.cm^{-2}), emission spectra (recorded every 3 s) after switching on the laser initially showed only weak phosphorescence of **1** at 800 nm and no upconversion emission (Figure 8.4a, inset). However, after 1 min of red light irradiation, the phosphorescence at 800 nm suddenly intensified and intense upconversion emission at 474 nm was observed. We define the progressed time until this time-point as the "lag-time" (see Figure 8.4a, inset). After 2 min, the emission spectrum had stabilized in time and it was identical to that observed under deoxygenated conditions (see Chapter 6, Figure 6.2). No upconversion was observed in air in absence of L-Asc (data not shown). To explain this observation, it was hypothesized that upon irradiation compound

1 first reacted with ground-state oxygen to make singlet oxygen, that in turn reacted with L-Asc. This photoreaction was repeated until all ground-state oxygen present in the irradiated solution was depleted. When the oxygen concentration becomes low enough, triplet-state photosensitizer and annihilator are no longer quenched, leading to efficient TTA-UC and increased phosphorescence of **1**.

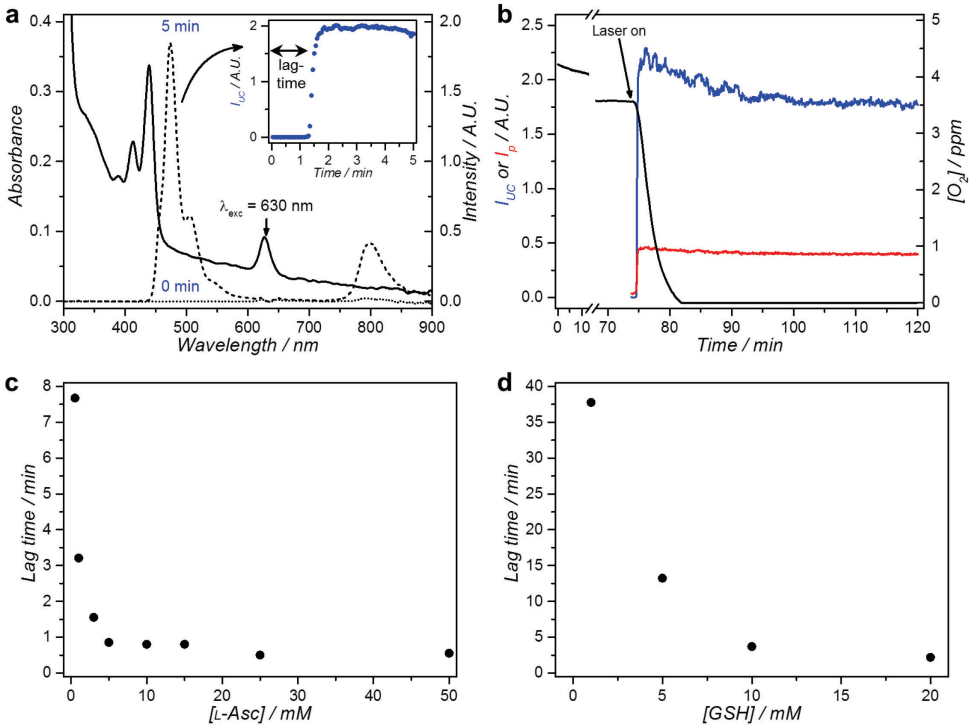

*Figure 8.4. Emission spectroscopy in air of **L1-2** liposomes PBS supplemented with L-Asc or GSH. a) Absorption (solid) and emission spectra (dotted: t = 0; dashed: t = 5 min) of **L1-2** liposomes in PBS supplemented with 5 mM L-Asc. Inset shows the upconversion intensity (I_{UC} at 474 nm) for the first 5 min of irradiation with 3 s intervals. b) Time trace of the upconversion intensity (I_{UC} at 474 nm, blue), phosphorescence intensity (I_p at 800 nm, red), and dissolved oxygen concentration (black) during red light irradiation of **L1-2** liposomes in PBS supplemented with 5 mM L-Asc. The laser was turned on after 74 min in the dark, as indicated by the arrow. c/d) Lag-time as a function of [L-Asc] (c) or [GSH] (d). Exp. conditions: [DLPC] = 1 mM, [**1**] = 0.5 μM, [**2**] = 5 μM, 2.25 mL sample, T = 20 °C 10 mW 630 nm laser excitation (80 mW.cm^{-2}) with approximately 8% of the volume simultaneously irradiated, pH 7.0 – 7.6.*

To confirm this hypothesis, the experiment was repeated while measuring the dissolved oxygen concentration using a NeoFox oxygen probe dipped in the solution (Figure 8.4b). In the first 74 min the sample was left in the dark and the oxygen concentration remained close to the initial value, showing that

ground state O_2 quenching is very slow with L-Asc. When the laser was turned on however, rapid consumption of all the oxygen in the cuvette was observed within 5 min while intense upconversion emission was observed after 1 min of continuous irradiation. The upconversion was stable for the next 45 min after which the experiment was stopped. Overall, these results demonstrate that the addition of L-Asc to a dispersion of upconverting liposomes allows efficient and stable upconversion to occur in air due to singlet-oxygen consumption upon irradiation.

To study whether the lag-time varies with anti-oxidant concentration, the experiment was repeated with [L-Asc] ranging from 0.25 to 50 mM and the lag-time was measured in each situation (Figure 8.4c). Noteworthy a concentration of 0.25 mM did not give rise to any upconversion, presumably because the concentration of oxygen in air-equilibrated water has about the same value (9 ppm; ~0.25 mM). Upon increasing [L-Asc] from 0.5 mM to 5.0 mM, the lag-time strongly decreased from 8 min to 1 min and had a value of ca. 0.5 min at a concentration of 50 mM. The same experiments were performed with GSH as anti-oxidant at 1 – 20 mM concentrations (Figure 8.4d), which is close to physiological concentrations of this biological anti-oxidant (0.5 – 10 mM).[5] For all concentrations, intense upconversion was also observed after a certain lag-time, but the lag-times were significantly longer than with L-Asc. Finally, a combination of 1 mM L-Asc and 5 mM GSH was used as anti-oxidant "cocktail". Stable upconversion was observed after 1.1 min, which is significantly faster than either of the anti-oxidants alone (3.2 min for [L-Asc] at 1 mM; 13 min for [GSH] at 5 mM). This result suggests that using a combination of L-Asc and GSH synergistically minimizes the lag-time. For this reason, in further experiments a combination of these two anti-oxidants was used. In conclusion, it was demonstrated that the addition of biologically relevant concentrations of biological anti-oxidants to upconverting liposomes results in stable TTA-UC in air-equilibrated solutions. Unfortunately, **L1-2** liposomes were found to be unsuitable for *in-vitro* experiments, due to high cytotoxicity of the PEGylated DLPC liposomes in preliminary experiments: when A549 lung carcinoma cells were incubated with **L1-2** liposomes ([DLPC] = 0.5 mM) for 4 h, 100% cell death was observed (data not shown). In contrast, DMPC liposomes were much less toxic and selected for the *in vitro* experiments (see below).

8.2.3 Anti-oxidants protect TTA-UC for DMPC liposomes *in vitro*

To investigate whether the addition of anti-oxidants would also enhance TTA-UC in cells, A549 lung carcinoma cells were grown *in vitro* and incubated with upconverting DMPC liposomes **M1-3** for 24 h with or without an anti-oxidant "cocktail" composed of 2 mM L-Asc and 2 mM GSH. Perylene (compound **2**) was replaced by 2,5,8,11-tetra(*tert*-butyl)perylene (compound **3**) to avoid partitioning of the annihilator to the water phase, which is known to occur for normal perylene.[6] Indeed, it was found that tert-butylation prevented liposomal escape of **3** (see Appendix VII for data and discussion). These experiments also confirmed that compound **1** does not escape from liposomes. After 24 h incubation and removing the excess of liposomes, the cells were imaged in bright field mode, with 405 nm, and with 639 nm excitation (2.7 and 26 $W.cm^{-2}$ intensity, respectively). Additionally, a 1% oxygen atmosphere was used to mimic median tumor oxygen partial pressures, which generally range from 0.5% to 4% (pO_2 = 5 – 30 mm Hg).[7] Using 405 nm excitation compound **3** was excited directly, leading to normal fluorescence. In this mode numerous fluorescent spots were observed throughout the cell cytoplasm, indicating that the liposomes had been successfully taken up. The presence of anti-oxidants did not influence the uptake of the vesicles. In absence of anti-oxidants, 639 nm excitation did not lead to significant upconversion luminescence, indicating that the liposomes were not capable of producing upconversion. However, when the cells were co-incubated with the anti-oxidant cocktail, bright upconversion was observed at the same sites as that of the fluorescence observed under 405 nm excitation. This result indicates that at these locations, both dyes were present simultaneously, thus suggesting that the liposomes were intact and functional. Note that under these conditions the upconversion luminescence was not very stable: it quickly faded and disappeared within a few seconds. Overall, these results demonstrate that co-treatment of cells with biologically relevant amounts of anti-oxidants can significantly boost upconversion of **M1-3** liposomes *in vitro*.

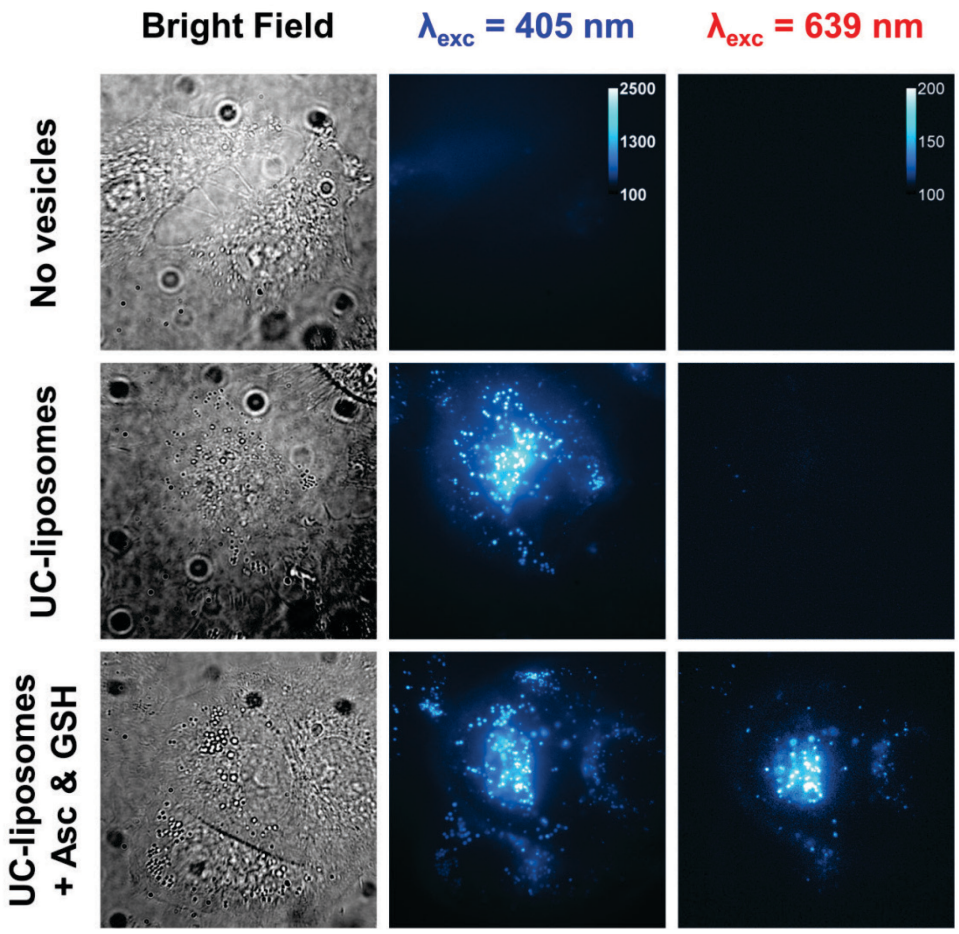

*Figure 8.5. In vitro upconversion imaging of **M1-3** upconverting liposomes in living A549 lung carcinoma cells in bright field mode (left column), with λ_{exc} = 405 nm and λ_{em} = 450 – 525 nm (middle column), and with λ_{exc} = 635 nm and λ_{em} = 450 – 525 nm (right column) at 100x magnification. Cells were incubated for 24 h with medium only (top row), with **M1-3** liposomes (middle row, [DMPC] = 1 mM), or **M1-3** liposomes with addition of 2 mM L-Asc and 2 mM GSH (bottom row, [DMPC] = 1 mM). Imaging conditions: T = 37 °C, 7.0% CO_2, 1.0% O_2, 75 µW 405 nm laser power (60 µm spot diameter, 2.7 W.cm^{-2} intensity), 1.0 mW 639 nm laser power (70 µm spot diameter, 26 W.cm^{-2} intensity). For comparability, the images are identically colored for λ_{exc} = 405 nm from 100 – 2500 pixel values (black → blue → white) , and for λ_{exc} = 635 nm from 100 – 200 pixel values (black → blue → white), as indicated by the calibration bars in the top row.*

To investigate the exact location of **M1-3** liposomes, the cells were additionally stained with LysoTracker Red DND-99 to label acidic organelles such as late endosomes and lysosomes. This probe is not excited with either 405 or 639 nm (Figure S.VII.2), and therefore does not interfere with the

fluorescence and upconversion luminescence imaging. Although live-cell colocalization was challenging due to the rapid movement of some of the fluorescent sites, images were successfully acquired in bright field mode, and with 405, 561, and 639 nm excitation when excitation sources were quickly changed (Figure 8.6). It was found that prompt fluorescence of compound **3** (λ_{exc} = 405 nm), upconversion luminescence (λ_{exc} = 639 nm), and LysoTracker Red fluorescence (λ_{exc} = 561 nm) all co-localized centrally in the cytosol. This colocalization indicates that the upconverting liposomes are present in acidic vesicles inside the cell. Therefore, **M1-3** liposomes are probably taken up by endocytosis and accumulate in late endosomes and lysosomes.

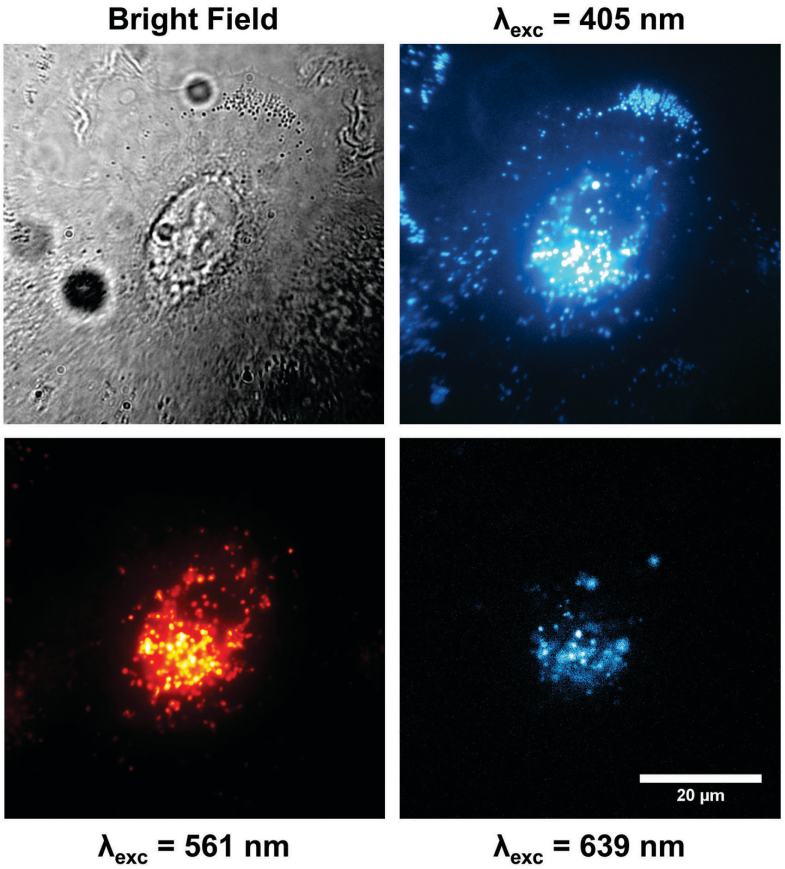

*Figure 8.6. In vitro imaging of **M1-3** liposomes in living A549 cells that were additionally stained with LysoTracker Red DND 99 in bright field mode, with λ_{exc} = 405 nm (to excite compound **3**), with λ_{exc} = 561 nm (to excite LysoTracker), and with λ_{exc} = 639 nm to generate TTA-UC (λ_{em} = 450 – 525 nm) at 1 % O_2. The cells had been incubated for 24 h with **M1-3** and anti-oxidants prior to imaging ([DMPC] = 1 mM, [L-ascorbate] =[GSH] = 5 mM). Same imaging conditions as in Figure 8.5.*

Curiously, upconversion was not observed at all locations where fluorescence of compound **3** was observed (Figure 8.5 and Figure 8.6). Whereas upconversion luminescence was especially located around the nucleus, the peripheral sites showing fluorescence of **3** did not produce any detectable upconversion. The peripheral fluorescence sites were found to be strongly clustered, strongly contrasting in bright-field mode, and not stained by LysoTracker Red (Figure 8.6). Furthermore, their size and location closely resemble that of lipid droplets[I] in HeLa and A549 cells.[8] We thus propose that compound **3** accumulates in lipid droplets after the digestion of the liposomes in lysosomes. The fact that the lipid droplets do not produce upconversion may be due to separation of **1** and **3** after liposome digestion, or because the local oxygen concentration in the lipid droplets is higher compared to endo- and lysosomes and TTA-UC is quenched. To investigate the latter hypothesis, cells were first treated with liposomes in absence of anti-oxidants. Then, instead of using singlet-oxygen scavengers, the cells were imaged in presence of 100 mM sodium sulfite (neutralized to *pH* 7) as ground-state oxygen to effectively deoxygenate the entire medium. Although many cells did not survive this treatment because of the dramatic increase in osmotic pressure, some cells could be successfully imaged before their death (Figure 8.7). The images strongly resemble the situation where the cells were co-treated with L-Asc and GSH: both the acidic organelles and the lipid droplets exhibit fluorescence of **3** (λ_{exc} = 405 nm), but upconverted emission (λ_{exc} = 639 nm) was only observed centrally in the cell. This result indicates that upconversion cannot be realized at any oxygenation level in the lipid droplets, and that compounds **1** and **3** must be physically separated and/or that compound **1** is degraded during digestion of the liposomes.

[I] Lipid droplets are the cell's organelles for lipid storage and metabolism.

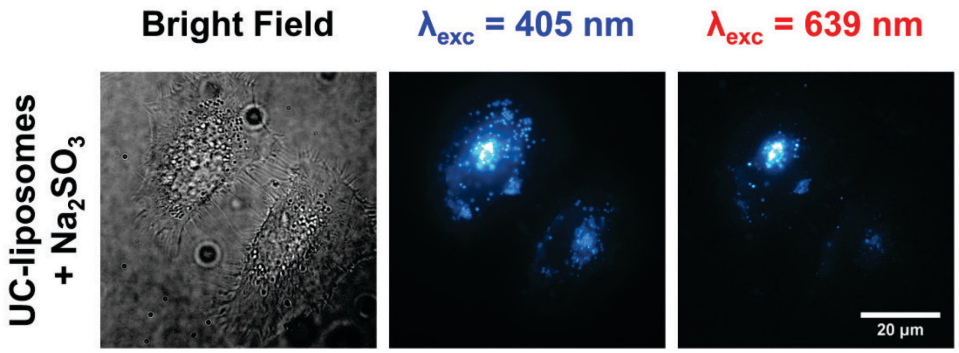

*Figure 8.7. In vitro imaging of **M1-3** liposomes in living A549 cells in bright field mode (left), with λ_{exc} = 405 (middle), and with λ_{exc} = 639 nm (right). After 24 h incubation with **M1-3** liposomes, the medium was refreshed, and the cells were imaged at 37 °C, 20% O_2 and 7% CO_2. Just before recording these images, 100 mM Na_2SO_3 in PBS (pH 7) was added to deoxygenate the medium. Other imaging conditions as in Figure 8.5.*

8.2.4 Cytotoxicity of upconverting DMPC liposomes with red light irradiation

It has been reported that photosensitizer **1** generates singlet oxygen upon red-light irradiation,[9] which is a highly cytotoxic species. In fact, singlet-oxygen generating photosensitizers are frequently used in photodynamic therapy (PDT) type II to kill cancer cells. Thus, it was anticipated that irradiation of **M1-3** liposomes inside living cells may lead to cell death. Therefore, the toxicity of upconverting DMPC liposomes was evaluated in the dark and upon red-light irradiation by treating three cell lines with **M1-3** liposomes according to a recently published (photo)cytotoxicity protocol developed in our group.[10] The cell lines used for this study were A549 (human lung carcinoma), MCF7 (human breast adenocarcinoma) and MRC5 (normal human lung) cells. As controls, **M1** (doped with only the photosensitizer) and **M3** (doped with only the annihilator) liposomes were used. In short, the photocytotoxicity protocol involved incubation of the cells with the liposomes for 24 h, after which the medium was refreshed and the cells were either irradiated in normoxic conditions (7% CO_2, 20% O_2, 37 °C) with high-power red light (628 nm, 23.0 ± 1.5 mW, 15 min, 20.7 J.cm^{-2}) or kept in the dark in otherwise identical conditions. The viability of the cells 48 h after irradiation was quantified with a sulforhodamine B staining assay. Prior to these experiments, the uptake of **M3** and **M1-3** liposomes after 24 h incubation was verified by imaging the fluorescence of **3** in the cells by fluorescence microscopy (λ_{exc} = 377 nm, Figure S.VII.3 and Figure S.VII.4). Because compound **1** is not emissive under these conditions, the uptake of **M1**

liposomes could not be visualized and we assumed that the uptake of **M1** is similar to the uptake of **M3**.

Figure 8.8 shows the evolution of cell viability as a function of the liposome concentration, expressed as the bulk concentration of DMPC (in mM) or compound **1** (in nM). In dark conditions, the data showed a limited decrease in cell viability of A549 and MCF7 cells treated with increasing liposome concentration, while the MRC5 cells were unaffected at any liposome concentration tested. This dark cytotoxicity can be explained by a lipid overdose at higher concentrations (> 100 μM). However, such high liposome concentrations are probably not clinically relevant[II] and it can thus be concluded that upconverting liposomes **M1-3** are non-toxic in the dark. Following red light irradiation, the dose-response curves were found to be very similar to those obtained in dark conditions. This result is surprising, as the experiments were carried out in a 20% O_2 atmosphere where PDT effects were expected. Apparently, the amount of singlet oxygen generated is too low to induce a cytotoxic effect. We attribute the low amount of singlet oxygen generation to the much lower photosensitizer dye doping (~0.05 mol% with respect to the lipid) compared to published liposomal PDT studies. For instance, one study reports M5076 ovarian sarcoma cells incubated with photofrin-loaded liposomes (8 mol% photofrin with respect to lipid) for 1 h[III] and exposed to 2 J.cm^{-2} 630 nm light;[13] this treatment caused approximately 50% cell death at a photofrin bulk concentration of 9 nM. Other explanations for the absent PDT effect may be: (i) the amount of endocytosed liposomes is too low to import enough photosensitizer; (ii) singlet oxygen that is generated in endo- and lysosomes may be less harmful compared to other cellular targets such as the mitochondria;[14] (iii) or the photosensitizer may be bleached before a significant amount of singlet oxygen is produced. Overall, our results clearly show that **M1-3** liposomes are not (photo)cytotoxic below

[II] Two clinically used liposomal anti-cancer drug formulations are Lipoplatin™ (9:91 w/w% cisplatin/lipid) and Doxil (11:89 w/w% doxorubicin/lipid).[11] The recommended dose of Lipoplatin™ is 200 mg.m^{-2} body surface area per 14 days. Given an average human body surface of 1.7 m^2, this leads to a dose of 309 mg lipids. At about 5 L of blood volume, the lipid in blood concentration would be 62 mg.L^{-1} (~ 85 μM). The recommended dose of Doxil is 50 mg/m^2 doxorubicin. Using the same figures, the lipid in blood concentration directly after administration would be 0.17 mM. These calculations suggest that lipid concentrations higher than ~0.1 mM, for which **M1-3** starts to become toxic, are probably not relevant for clinical application. Furthermore, liposome uptake studies in mice from the late 1980s and early 1990s report concentrations of 0.1 – 0.7 mM (in blood circulation directly after injection).[12]

[III] The authors do not mention refreshment of the medium before irradiation.

0.1 mM [DMPC] in the dark and under a high dose of red-light irradiation (20.7 J.cm^{-2}) in both cancer cells and healthy cells.

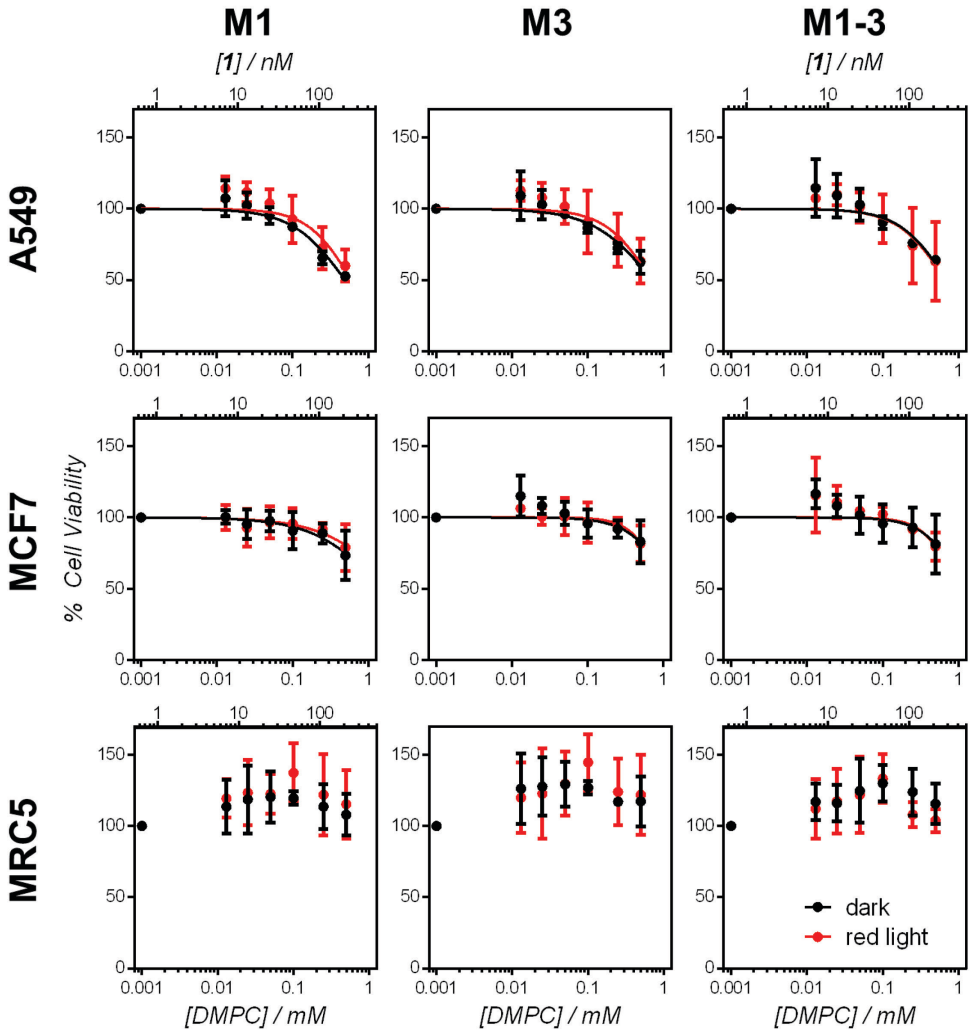

*Figure 8.8. Cell viability of A549 (top row), MCF7 (middle row) and MRC5 cells (bottom row) treated with **M1** (left column), **M3** (middle column), or **M1-3** liposomes (right column) and left in the dark (black data points) or irradiated for 15 min with 628 nm light (red data points, 20.7 J.cm^{-2} light dose) as a function of [DMPC] (bottom axes) or [**1**] (top axes). Solid lines represent Hill-slope fit curves to the same color data points. Error bars represent the standard deviation of the mean cell viability value from three individual biological experiments.*

8.2.5 Anchoring amphiphilic Ru-complexes to DMPC liposomes

After establishing the photophysical properties and low cytotoxicity of the upconverting liposomes (System A), the photocytotoxicity of Ru-complex

functionalized liposomes (System B) irradiated with blue light in absence of upconversion was considered. Four Ru-complexes were investigated for use in System B: compounds $\mathbf{4}^{2+}$, $\mathbf{5}^{2+}$, $\mathbf{6}^{2+}$, and $\mathbf{7}^{2+}$ (Figure 8.2). These compounds all dissolve poorly in water, and feature a cationic Ru^{2+} compound functionalized with a lipophilic ligand (cholesterol-thioether in $\mathbf{4}^{2+}$, alkyl-thioether in $\mathbf{5}^{2+}$ and $\mathbf{6}^{2+}$, and double alkyl-tailed neocuproine in $\mathbf{7}^{2+}$). Each of these compounds is non-emissive (Φ_{em} << 1%) and photodissociative: upon blue-light irradiation in water, compounds $\mathbf{4}^{2+}$ and $\mathbf{5}^{2+}$ react to mono-aqua product $[Ru(tpy)(bpy)(H_2O)]^{2+}$ (compound $\mathbf{8}^{2+}$),[15] and compounds $\mathbf{6}^{2+}$ and $\mathbf{7}^{2+}$ react to bis-aqua product $[Ru(bpy)_2(H_2O)_2]^{2+}$ (compound $\mathbf{9}^{2+}$; see Figure S.VII.6 to Figure S.VII.8). In presence of liposomes, these compounds insert in the membrane and upon blue-light irradiation the photoproduct dissociates from the membrane as illustrated in Figure 8.9a.[16] Thus, PEGylated DMPC liposomes were functionalized with 4 mol% $\mathbf{4}^{2+}$, $\mathbf{5}^{2+}$, $\mathbf{6}^{2+}$, or $\mathbf{7}^{2+}$ (**M4**, **M5**, **M6**, and **M7** respectively). In spite of the lipophilic anchor ligands it was initially uncertain whether the Ru complexes were adequately anchored and would not escape the membrane over time in the dark. In an *in vivo* situation, such "hopping" would mean that in the dark the Ru-complex would escape the liposome drug carrier and insert in biological membranes, *i.e.* before the tumor site is reached, leading to poor selectivity and to potential side-effects.

To investigate whether or not hopping of the complexes from one membrane to another occurs, a simple but effective assay was developed, illustrated in Figure 8.9b. In short, **M4**, **M5**, **M6**, or **M7** liposomes were added to a stirred solution of **M3** liposomes while measuring the fluorescence intensity of **3** (λ_{exc} = 420 nm, λ_{em} = 486 nm). As discussed in Appendix VII, **3** does not hop from membrane to membrane. Compounds $\mathbf{4}^{2+}$, $\mathbf{5}^{2+}$, $\mathbf{6}^{2+}$, and $\mathbf{7}^{2+}$ all have substantial absorbance overlap with the emission of **3** (Figure S.VII.5), so that FRET occurs if the Ru complexes come in close proximity of **3**, as was reported in Chapter 4.[4b] Also, fusion of the liposomes does not spontaneously occur (no changes in DLS were observed upon mixing), and close liposomal proximity is prevented because both liposome samples are sterically hindered with PEG groups.

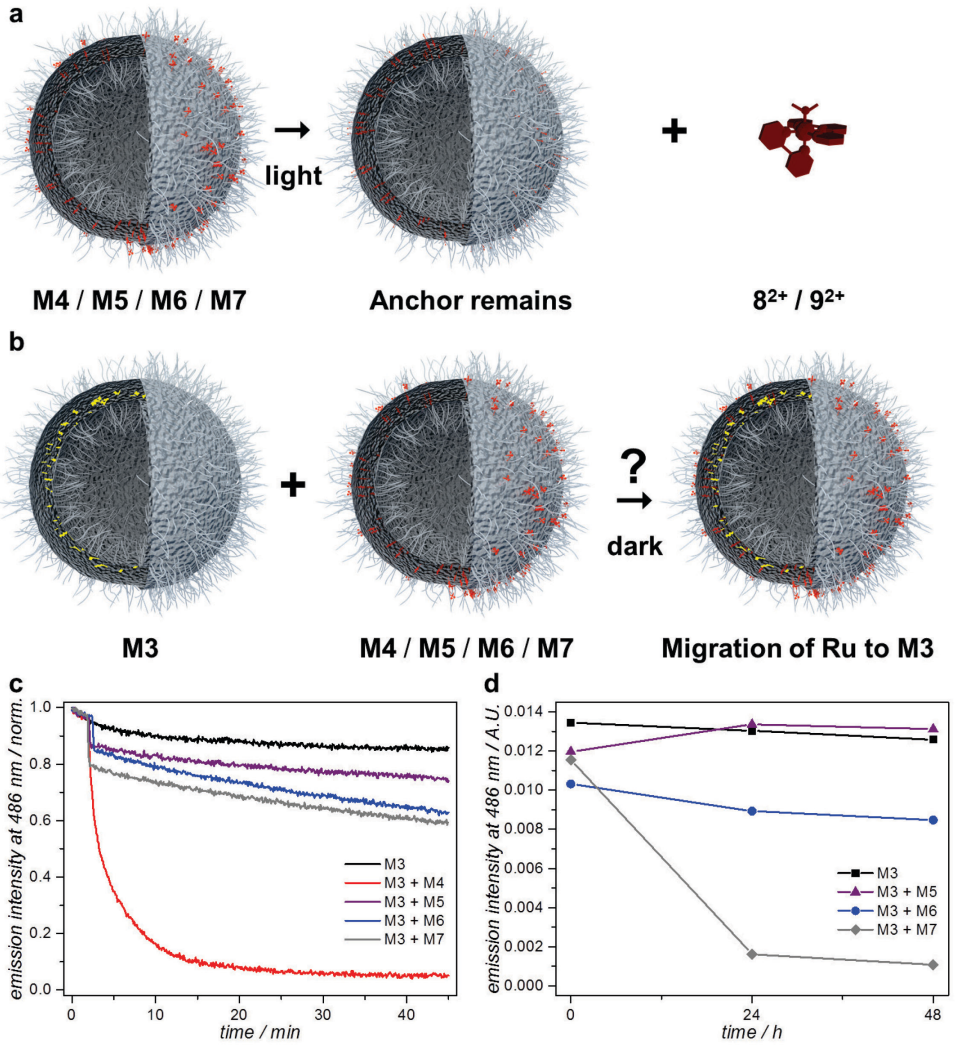

Figure 8.9. Fluorescence assay to determine "hopping" of Ru-complexes ***4***$^{2+}$, ***5***$^{2+}$, ***6***$^{2+}$, *and* ***7***$^{2+}$ *from liposome to liposome. a) Cartoon illustrating the photodissociation reaction of a Ru complex that is anchored to a liposome with a lipophilic ligand: upon irradiation the photoproduct dissociates while the anchor remains (here* ***4***$^{2+}$ *reacts to* ***8***$^{2+}$*). b) Cartoon of the hopping process. c/d) Fluorescence emission intensity of* ***3*** *at 486 nm (*λ_{exc} *= 420 nm, 240 µW.cm*$^{-2}$ *intensity) as a function of time after mixing liposomes* ***M3*** *with* ***M4***, ***M5***, ***M6***, *or* ***M7*** *for the first 45 min (c) and for 24 h and 48 h after mixing (d). In part (c), the Ru-doped liposomes were added at t = 2 min. Conditions: 2 mL volume in a stirred macro cuvette at 20 °C, [DMPC] = 50 µM of each liposome formulation,* ***[3]*** *= 0.25 µM.*

In Figure 8.9 the fluorescence intensity of **3** as a function of time after mixing is shown. While the fluorescence intensity in the mixtures of **M3** and **M5**, **M3** and **M6**, or **M3** and **M7** stayed relatively stable with time, the fluorescence

intensity of **3** in the mixture of **M3** and **M4** rapidly decreased within the first 20 minutes after mixing and was quenched by 95% after 45 min. Negligible reduction in fluorescence was observed for **M3** without any addition. It is thus very clear that $\mathbf{4}^{2+}$ is inadequately trapped in **M4** liposomes and readily equilibrates with the membrane of **M3** within the first 45 minutes of mixing. The other Ru complexes seem to be tightly anchored to the liposomes, at least during the first 45 min. In a further experiment, the fluorescence of **3** in these mixtures was measured 24 and 48 h after mixing (Figure 8.9b). The fluorescence intensity of **3** in the mixtures of **M3** and **M5**, and **M3** and **M6** was again very stable, but it decreased greatly for the mixture of **M3** and **M7** (~90% quenching after 48 h). Thus, $\mathbf{7}^{2+}$ also hops from membrane to membrane, but slower than $\mathbf{4}^{2+}$. These results imply that it is not straightforward to synthesize a lipophilic anchor to trap an inorganic Ru-complex to a liposome. For $\mathbf{3}^{2+}$ we attribute the escape to the PEG_3-cholesterol moiety of $\mathbf{3}^{2+}$ being not lipophilic enough. However, it was surprising to find that a double-tail alkyl ligand ($\mathbf{7}^{2+}$) is not a strong anchor, while a single-tail alkyl ligand is. Overall, it was found that under these conditions, complexes $\mathbf{5}^{2+}$ and $\mathbf{6}^{2+}$ are well-trapped in the lipid bilayer of **M5** and **M6**, so that these complexes were considered as suitable candidates for further biological experiments. Complexes $\mathbf{4}^{2+}$ and $\mathbf{7}^{2+}$ were excluded from biological experiments.

8.2.6 Photo(cytotoxicity) of Ru-complex doped liposomes under blue light irradiation

As introduced earlier, the purpose of Ru-complex doped liposomes (System B) is to transport the Ru-complex inside the cell, after which the complex can be activated with blue light to produce a toxic aqua species (complex $\mathbf{8}^{2+}$ or $\mathbf{9}^{2+}$, see Figure 8.2). To test this hypothesis, the (photo)cytotoxicity of **M5** and **M6** liposomes was evaluated in A549, MCF7, and MRC5 cells according to the same protocol that was used before for **M1-3** liposomes (Section 8.2.4). However, instead of using red light the cells were this time irradiated for 10 minutes with a 454 nm LED-array (7.0 ± 0.8 $mW.cm^{-2}$ intensity, 4.2 $J.cm^{-2}$ dose) under 7% CO_2 and 20% O_2. It was previously found that a longer irradiation time may cause significant cell death.[17] As complexes $\mathbf{5}^{2+}$ and $\mathbf{6}^{2+}$ are not emissive the uptake of the liposomes could not be confirmed by fluorescence microscopy. Furthermore, the activation half-time to convert $\mathbf{5}^{2+}$ to $\mathbf{8}^{2+}$ and $\mathbf{6}^{2+}$ to $\mathbf{9}^{2+}$ was estimated to be 3 min (see Appendix VII for calculation), so that in such conditions it was anticipated that 10 min

irradiation would nearly convert all of the complex to the aqua species. The evolution of cell viability as a function of concentration is shown in Figure 8.10, and the 50% effective concentration values (EC_{50}) and photo-indices (PI, calculated by $PI = EC_{50}^{dark} / EC_{50}^{light}$) are reported in Table 8.2.

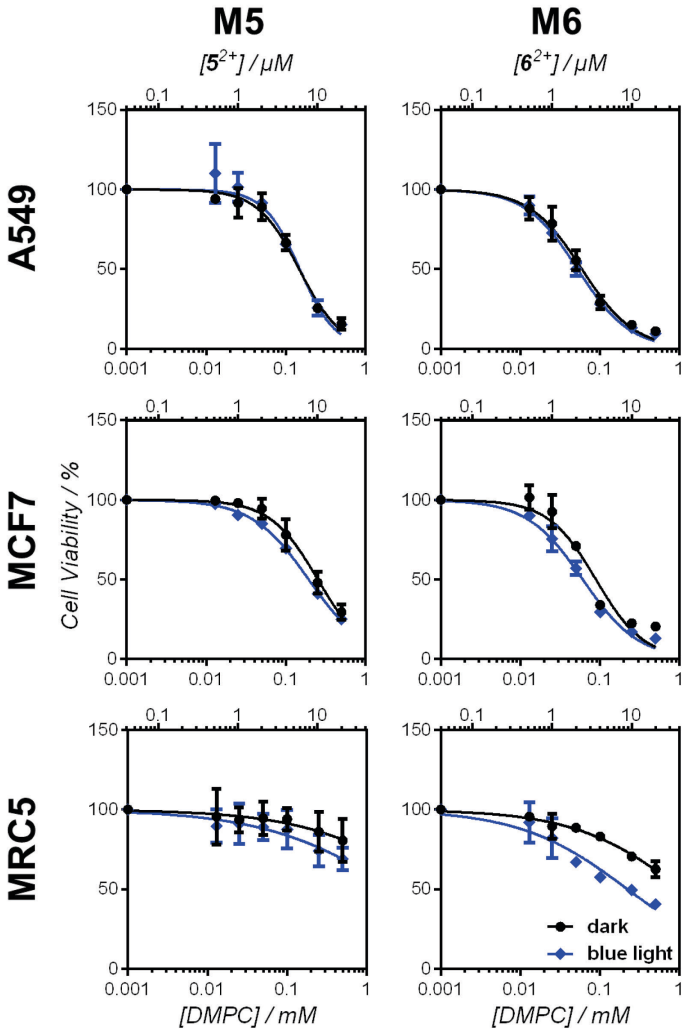

*Figure 8.10. Cell viability of A549 (top row), MCF7 (middle row) and MRC5 cells (bottom row) treated with **M5** (left column), or **M6** (right column) liposomes and left in the dark (black circles) or irradiated for 10 min with 454 nm light (blue diamonds, 4.2 J.cm⁻² light dose) as a function of [DMPC] (bottom axes) or [Ru] (top axes). Solid lines represent Hill-slope fit curves to the same color data points. Error bars represent the standard deviation of the mean cell viability value from three individual biological experiments.*

*Table 8.2. EC_{50} values (expressed in μM [Ru]; [Ru] = 0.04 × [DMPC]) and photo-indices (PI) of **M5** and **M6** liposomes after irradiation with 454 nm light (10 min, 7.0 ± 0.8 mW.cm^{-2} intensity, 4.2 J.cm^{-2}) and in the dark in A549, MCF7 and MRC5 cells. Confidence intervals (CI) are given in μM.*

Cell line	Light	**M5**				**M6**			
		EC_{50} (μM)	CI (μM) -	CI (μM) +	PI	EC_{50}	CI (μM) -	CI (μM) +	PI
A549	+	6.0	1.1	1.4	1.0	2.1	0.2	0.2	1.1
	-	5.9	0.8	0.9		2.4	0.3	0.4	
MCF7	+	7.8	0.6	0.6	1.3	2.4	0.3	0.4	1.5
	-	10	1.3	1.5		3.6	0.8	1.0	
MRC5	+	93	76	410	3.0	8.9	2.8	4.0	4.8
	-	270	270	15E3		43	13	20	

The data show that both **M5** and **M6** liposomes are toxic for A549 cells in the dark with EC_{50} values of 5.9 and 2.4 μM [Ru], respectively. In both cases irradiation with blue light marginally affected the values. In MCF7 cells, **M5** and **M6** had EC_{50} values of 10 and 3.6 μM [Ru]; light irradiation slightly lowered these values to 7.8 and 2.4 μM [Ru], respectively. Finally, in MRC5 cells, **M5** and **M6** liposomes had EC_{50} values of 270 and 43 mM [Ru], respectively, which shows that the liposomes barely affect MRC5 cells in the dark. However, light irradiation lowered the EC_{50} values to 93 and 8.9 μM [Ru], respectively, which is statistically significant. Unfortunately the photo-indices of both liposome-bound complexes were rather low. Overall, the data show that **M5** and **M6** are more toxic in the dark than **M1-3** liposomes (compare Figure 8.10 to Figure 8.8), clearly indicating that **5**$^{2+}$ and **6**$^{2+}$ are toxic in the dark. What is the origin of this toxicity? Since the surface of the liposomes is sterically hindered with PEG groups, the interaction of the membrane-bound complex with biomolecules of the cell is hindered. Another possibility is that toxic interactions arise after digestion of the liposomes, after which **5**$^{2+}$ or **6**$^{2+}$ is liberated. In such a scenario, even though **5**$^{2+}$ and **6**$^{2+}$ are not photoactivated, their amphiphilicity may in fact cause significant toxicity. For instance, it has recently been shown that complex **4**$^{2+}$ in absence of liposomes and in the dark is significantly toxic in A549 and MCF7 cells with a EC_{50} value of 5 μM, comparable to the data of **M5** and **M6**.[18] If liposome digestion is indeed the cause of the dark toxicity, drug carriers with higher resistance towards digestion may be needed to lower the dark toxicity. Interestingly, the data also show that **M5** and **M6** are more toxic for cancerous cells (A549 and MCF7) than for healthy cells (MRC5). This observation may indicate a selectivity of liposome-bound complexes **5**$^{2+}$ and **6**$^{2+}$ for cancer cell lines. Thus,

blue light irradiation can generally cause more cell death, but that this effect is highly cell-dependent. In the rest of this chapter, complex $\mathbf{6}^{2+}$ is used as Ru prodrug, because it exhibits the greatest photo-index.

8.2.7 Activation of a photodissociative ruthenium complex using upconverting DMPC liposomes in air

As introduced earlier, the photoreaction of $\mathbf{6}^{2+}$ can only be executed efficiently using blue light. In Chapter 4 it was demonstrated that in liposomes that were doped with compounds **1**, **2**, and $\mathbf{4}^{2+}$, the upconverted light was efficiently transferred to the ruthenium complex via FRET and triggered the photodissociation of the complex. However, those experiments were performed under deoxygenated conditions (by bubbling the solution with argon) and the red light activation did not work in air, which clearly limited the biological applicability of System C liposomes. On the other hand, as demonstrated in sections 8.2.2 and 8.2.3, anti-oxidants such as L-Asc and GSH protect TTA-UC against oxygen. An obvious step forward was thus to add anti-oxidants to System C liposomes in order to protect TTA-UC and trigger the photodissociation with red light in air. In such a mixture of anti-oxidants and TTA-UC-Ru liposomes, it is important to consider that the anti-oxidants may in fact interfere with the photosubstitution reaction of $\mathbf{6}^{2+}$ to $\mathbf{9}^{2+}$: for instance, anti-oxidants may react with ground or excited-state $\mathbf{6}^{2+}$ and cause unwanted side-reactions, or the thiol of GSH may substitute water in $\mathbf{9}^{2+}$ to form a GSH-Ru adduct. Thus, the influence of anti-oxidants on a TTA-UC-photodissociation reaction cascade had to be evaluated.

For this purpose, **M1-3-6** liposomes were prepared at 1 mM [DMPC] that contained red-to-blue TTA-UC compounds **1** and **3** and photodissociative Ru-compound $\mathbf{6}^{2+}$. The photodissociation reaction with red light irradiation was performed in either deoxygenated conditions by bubbling argon for 30 min, or in air-equilibrated conditions and in presence of 10 mM L-Asc and 10 mM GSH. Both samples were irradiated at human body temperature (37 °C) with 630 nm light (150 mW, 1.2 W.cm^{-2}) for 2.5 h while recording UV-vis absorbance (Figure 8.11a and b) and emission spectra every 15 min. The UV-vis spectrum at t = 0 shows the characteristic absorption bands of **1** at 440 and 630 nm, of **3** between 375 and 450 nm, while the absorbance of $\mathbf{6}^{2+}$ (Figure S.VII.7) is hidden under the bands of **1** and **3**. Under argon, in absence of anti-oxidants, the absorption band of the photoproduct $\mathbf{9}^{2+}$ evolves to completion in the first hour of irradiation, just as observed for complex $\mathbf{6}^{2+}$ in water upon blue light irradiation (Figure S.VII.7). By plotting the absorbance at 490 nm *versus* time

(Figure 8.11c), it is clear that the photoreaction was completed after about 45 min of irradiation. While the photoreaction was progressing, the upconversion emission at 486 nm increased (Figure 8.11d), because complex $\mathbf{9}^{2+}$ dissociates into solution and no longer quenches the emission of **3** via FRET (see Chapter 4). After 60 – 90 min of irradiation, both the absorption and emission spectra completely stabilized. When the experiment was conducted in air and in presence of anti-oxidants, the same absorption band between 460 and 600 nm appeared in the first 30 min of irradiation (Figure 8.11b), which strongly resembled the absorption band of $\mathbf{9}^{2+}$. After that time-point, this absorption band slowly disappeared, indicating that the photoproduct was not stable upon prolonged irradiation or further reacts with L-Asc and/or GSH. Also the upconversion emission intensity increased in the first two hours of irradiation, similar to the previous experiment. As control, the irradiation experiment under argon was repeated with **M3-6** liposomes, which did not contain photosensitizer **1** and hence could not produce TTA-UC. A slow evolution of the absorbance at 490 was observed, which is attributed to direct absorption of the red light by $\mathbf{6}^{2+}$. These results demonstrate that TTA-UC greatly amplified the rate of photodissociation upon red light irradiation. At these irradiation conditions, 45 min were necessary to activate 40 µmol ruthenium prodrug.

Is the same photoproduct obtained under argon and in air in presence of anti-oxidants? To answer this question, the irradiation experiments were repeated, but stopped after 60 min; the liposomes were removed from the solution using a centrifugal filtration, and UV-vis absorption spectra of the filtrates were recorded. In case of irradiation under argon, the UV-vis absorption spectrum of the filtrate was identical to the absorption spectrum of $\mathbf{9}^{2+}$ (Figure S.VII.7 and Figure S.VII.9), thereby confirming the photodissociation reaction of $\mathbf{6}^{2+}$ to $\mathbf{9}^{2+}$. In the presence of anti-oxidants, the resulting absorption spectrum was very similar, suggesting that the same (or a similar) Ru-complex had been formed. As control, no absorption was detected for filtered solutions of non-irradiated **M1-3-6** liposomes under argon or in presence of anti-oxidants. Finally, the same irradiation experiments were repeated at higher concentration (20 mM DMPC), and mass spectra were recorded after centrifugal filtration, lyophilisation of the filtrate, and redissolving the residue in acetone (Figure S.VII.10). In case of irradiation under argon, the mass spectrum confirmed that $\mathbf{9}^{2+}$ had indeed formed during irradiation (main peaks 490.1 and 507.1 m/z belonging to $[Ru(bpy)_2(OH_2)(OH)]^+$(MeCN) and

$[Ru(bpy)_2(OH_2)(OH)]^+$(acetone), respectively). In case of irradiation in air in presence of anti-oxidants, the sample only dissolved in methanol, which suggests that another Ru-complex had been formed. The mass spectrum showed 481.1 and 490.0 m/z, belonging to $[Ru(bpy)_2(OH_2)_2]^{2+}(MeO^-)$ and $[Ru(bpy)_2(OH_2)(OH)]^+(MeCN)$, see Figure S.VII.11. Although no signals were detected from a GSH complex, for example expected at m/z 738.1 for $[Ru(bpy)_2(GS)(H_2O)]^+$, it is still plausible that compound **9**$^{2+}$ and products such as GSH adducts co-exist in the reaction mixture. Overall, the results demonstrate that GSH and L-Asc facilitated the photoactivation cascade of TTA-UC, FRET, and Ru-photodissociation in air while minimally interfering with the photochemistry. These findings may thus be used to investigate Ru-prodrug activation using TTA-UC *in vitro*.

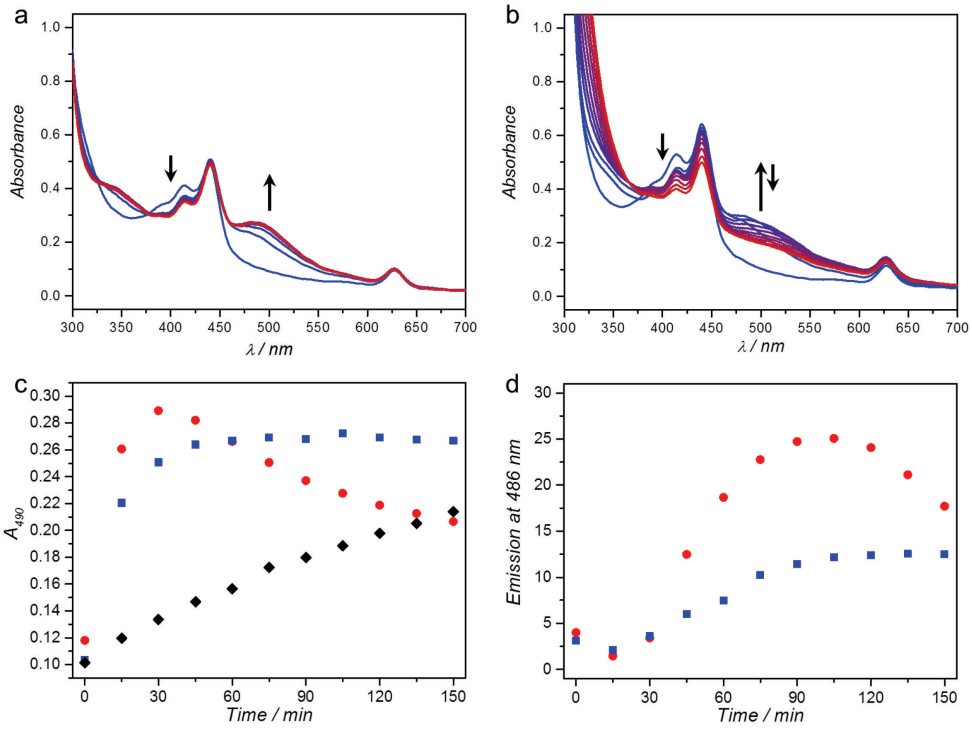

*Figure 8.11. a/b) UV-vis absorption spectroscopy in 15 min intervals (blue to red gradient) during red-light irradiation of **M1-3-6** liposomes under argon (a) and in air in presence of 10 mM L-Asc and GSH (b). c/d) Absorbance at 490 nm (c) and upconversion emission at 486 nm (d) as a function of time for the experiment under argon (blue squares) and in air in presence of anti-oxidants (red circles). As control, **M3-6** liposomes were irradiated under the same conditions under argon (c, black diamonds). Conditions: 2 mL sample with 1 mM DMPC, irradiated at 37 °C with 150 mW 630 nm light (1.2 W.cm^{-2}).*

8.2.8 Inducing TTA-UC and drug activation through meat with DLPC liposomes

The main reason to use red-to-blue light upconversion in PACT is the increased excitation penetration depth of red light in tissues. To study the activation of a ruthenium prodrug using red-to-blue TTA-UC in liposomes, a two-fold investigation was performed. First, the depth at which TTA-UC can be generated through biological tissues was measured for **L1-2** liposomes by placing layers of fresh meat (chicken or pig) between the excitation source and the sample. Secondly, the photodissociation of $\mathbf{6}^{2+}$ to $\mathbf{9}^{2+}$ with red light and **L1-3-6** liposomes was attempted through a layer of pork to simulate operation conditions.

In order to measure the depth at which red-to-blue upconversion can be generated through biological tissues, first an upconverting gel was prepared by mixing **L1-2** liposomes ([DLPC] = 10 mM) with 0.5 wt.% agarose and 5 mM L-Asc and GSH in PBS and was deposited as a thin disk between two microscopy slide. The gel was then covered with a variable stack of meat slices, a 630 nm laser beam (0.57 W.cm^{-2}) was directed through the meat at the upconverting gel, and the emission spectrum was measured of the sample in a custom-made cage spectroscopy setup (see experimental section, Figure 8.16). Raw chicken breast fillet and pork fillet were selected to mimic human tissue of different color and structure, and were thinly sliced with 1 – 2 mm thickness.

The emission spectra for both meat types showed the typical phosphorescence of **1** at 800 nm and upconversion emission of **2** at 474 nm identical to the emission spectra shown in section 8.2.2 (Figure 8.12a and c). As could be expected, the intensity of the entire spectrum decreased as a function of meat thickness due to filtering and scattering of the excitation source by the meat. In a typical experiment, upconversion was still observable for 12.8 mm thick chicken and for 11.6 mm thick pork. Figure 8.12c and d show the upconversion intensity (I_{UC}), the phosphorescence of **1** (I_p), and their ratio as a function of meat thickness. It can be clearly seen that from the third meat layer onwards, I_{UC} decreases relatively faster than I_p; *i.e.* I_{UC}/I_p decreases. This can be rationalized by the fact that TTA-UC is quadratically dependent on the excitation intensity below the intensity threshold for efficient upconversion (I_{th}), while the phosphorescence is linearly dependent. I_{th} was previously determined to be 0.05 W.cm^{-2} for very similar red-to-blue TTA-UC in DOPC liposomes (Chapter 5). Considering that I_{UC}/I_p changes for the first

time after 3 layers of meat, this must mean that the excitation intensity after 3 layers of meat has decreased from 0.57 W.cm^{-2} to approximately 0.05 W.cm^{-2}). Overall, the results show that upconversion was generated even beyond 1 cm penetration depth, but that beyond 5 to 6 mm meat depth the TTA-UC efficiency decreased quickly. Naturally, the depth at which the excitation intensity equals I_{th} depends on the initial excitation intensity, so it was decided that a higher irradiance was needed to activate Ru-prodrugs through meat (see below). Finally, the results also suggest that upconverting drug carriers should have a low I_{th} value, so that their performance would be minimally dependent on the excitation intensity.

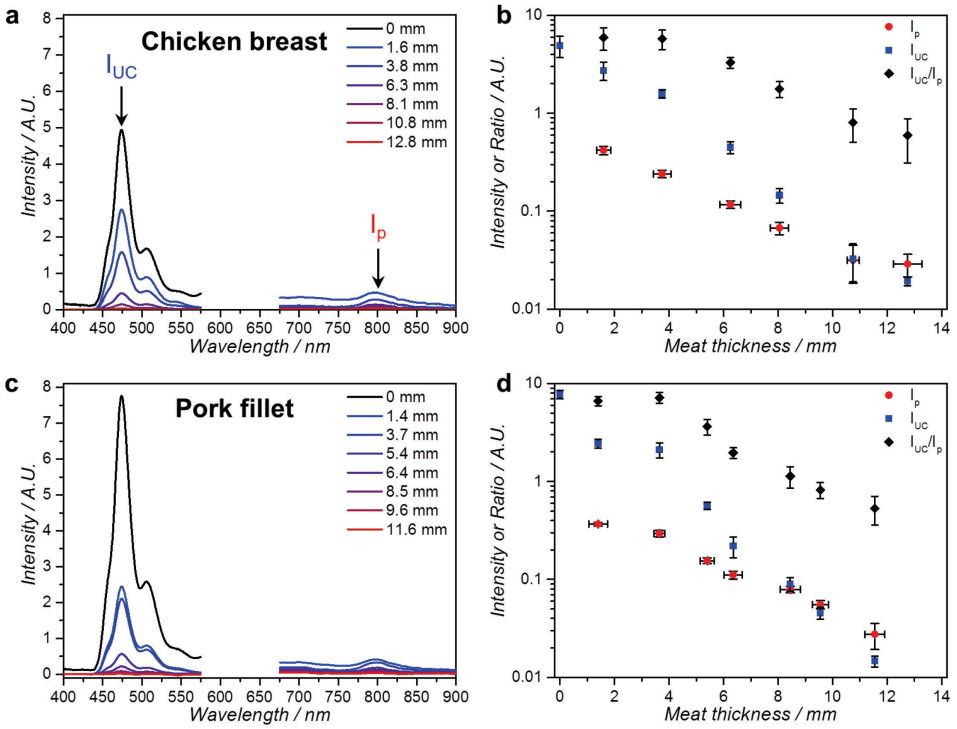

*Figure 8.12. Emission spectroscopy of an upconverting liposome gel through layers of chicken breast or pork fillet. a/c) Emission spectra of gellified **L1-2** liposomes through layers of meat at room temperature as a function of chicken breast (a) or pork fillet thickness (c). b/d) Upconversion intensity (I_{UC}, at 474 nm), phosphorescence intensity of compound **1** (I_p) and the ratio of I_{UC} and I_p as a function of chicken breast (b) or pork fillet (d) thickness. Conditions: 20 µL sample in a 25 µm × 25 mm diameter disk of **L1-2** liposomes ([DLPC] = 10 mM) in 0.5% wt.% agarose gel, 5 mM L-Asc, and 5 mM GSH in PBS at room temperature, irradiated with 30 mW (3 mm spot, 0.57 W.cm^{-2}) 630 nm light through a variable number of meat slices. The spectra are cut off between 575 nm and 675 nm to omit the large excitation scatter peak.*

The second set of experiments involved Ru-complex activation through a layer of meat. For this, a 2 mm thick cuvette was filled with 400 µL **L1-3-6** liposomes ([DLPC] = 10 mM) in anti-oxidant PBS (10 mM L-Asc and GSH), buried under a layer of pork fillet (7 ± 0.5 mm), and irradiated from the top with either red or blue light for 2 h, as shown in Figure 8.13a. The light dose was equal for both experiments (110 mW laser light, 3 mm spot size, 1.6 W.cm^{-2}, 11.2 kJ.cm^{-2}); higher intensity blue light could not be realized in our experimental setup. The UV-vis absorption spectrum of the cuvette (without meat) was measured before and after irradiation (Figure 8.13b). The absorption band that appeared between 460 and 600 nm indicated the formation of a small quantity of the aqua species **9**$^{2+}$ (compare Figure 8.11a and Figure 8.13b). The amount of activated Ru-complex was similar for both excitation wavelengths.

This result can be interpreted by considering the two different photochemical pathways of activation. In the case of blue light, the light does not penetrate the meat far, but the photons that do reach the sample have a high chance of being absorbed due to the high absorbance of **6**$^{2+}$ at 450 nm (ε_{450} ≈ 6000 M^{-1}.cm^{-1}, [**6**$^{2+}$] = 0.40 mM; $A_{450}^{\mathbf{6}^{2+}}$≈ 0.5 for 2 mm path length). Upon blue light absorption, the complex is directly activated without intervention of the TTA-UC process, i.e. the chance is high that a blue photon causes photodissociation of **6**$^{2+}$. In the case of red light, the light penetrates much further, *i.e.* more light reaches the cuvette, but the overall activation efficiency is the product of upconversion quantum yield (Φ_{UC}), energy transfer efficiency from annihilator **3** to Ru-complex **6**$^{2+}$ (E_{ET}), and photodissociation quantum yield (Φ_{Ru}; see Chapter 4),[4b] leading to a ~20 times lower overall activation efficiency. Also, the absorbance of compound **1** at 630 nm was comparatively low ($A_{630}^{\mathbf{1}}$ = 0.15), leading to less use of the light that permeates through the meat. Finally, at 1.6 W.cm^{-2} 630 nm excitation intensity, it is likely that Φ_{UC} is lower than its maximum value, because the excitation intensity likely drops to I_{th} or below (~0.05 W.cm^{-2}). Thus, even though **L1-3-6** liposomes are clearly more responsive to blue light, the data show that the overall activation with red light was approximately just as efficient as with blue light. Improvements in red-light absorbance and upconversion efficiency may eventually lead to a better performance with red light compared to blue light at this meat thickness.

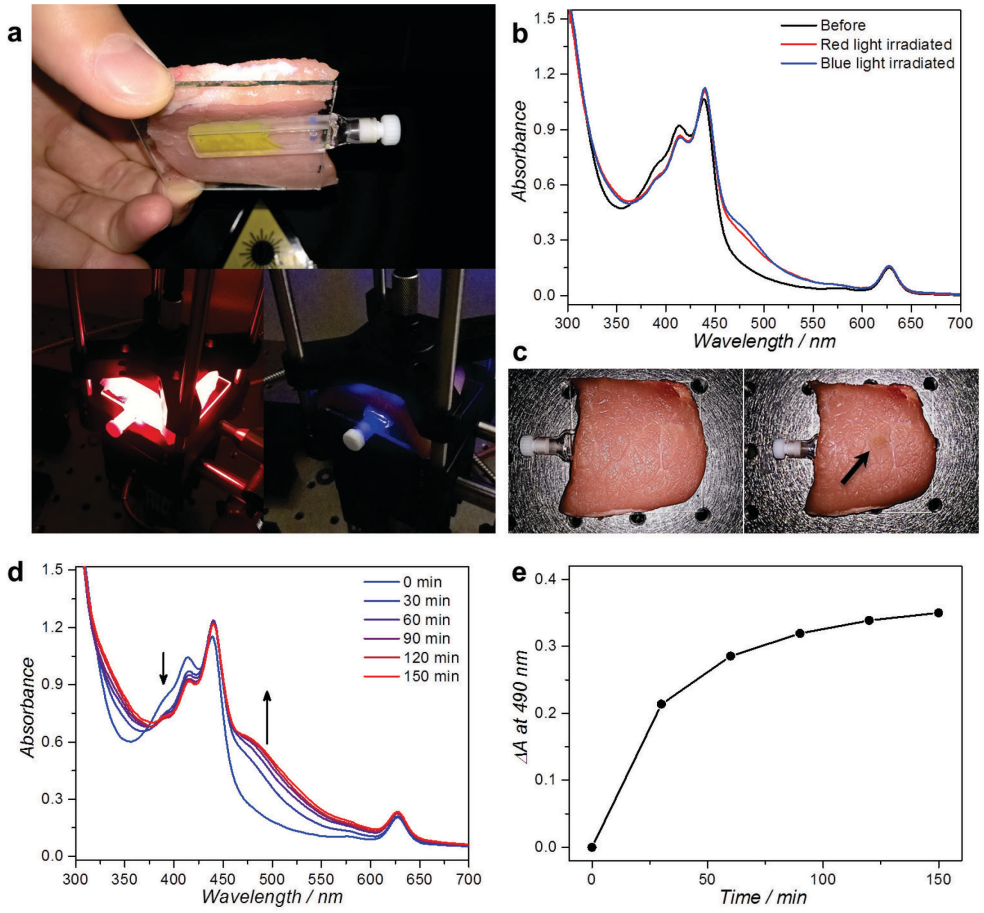

*Figure 8.13. Irradiation of **L1-3-6** liposomes through a thick slice of pork fillet. a) Photographs of the experimental setup used for red and blue light irradiation. The 2 mm cuvette holding 400 µL **L1-3-6** ([DLPC] = 10 mM) is covered with 7 mm pork fillet and irradiated for 2 h from above with a collimated 110 mW 630 or 450 nm beam (3 mm spot size, 1.6 W.cm^{-2} intensity, 11.2 kJ.cm^{-2} light dose). b) UV-vis absorbance spectra of the sample before (black) and after irradiation with 450 nm (blue) or 630 nm light (red). c) Photographs of the pork fillet after red (left) or blue light irradiation (right). Upon blue light irradiation, a clear "burn mark" was observed, as indicated with the arrow. d/e) UV-vis absorbance spectra (d) and the absorbance difference at 490 nm (e) as a function of irradiation time for **L1-3-6** liposomes irradiated through 7 mm pork fillet with 300 mW.cm^{-2} 630 nm light (4.2 W.cm^{-2}).*

Apart from investigating the sample after irradiation, the meat was also visually inspected after the 2 h irradiation. While red light had caused no damage at all, blue light had burned the meat considerably at the irradiation spot (Figure 8.13c). This result is consistent with data of our group that blue light is much more harmful for cells than green or red light.[10] Red light is thus much more favorable for drug activation than blue light. Tissue ablation is also

a great issue in the biological application of lanthanoid-based upconversion nanoparticles (UCNPs): for instance, it has been shown by Wu *et al.* that irradiation of chicken meat with 980 nm laser light for 20 min at ≥ 5 W.cm^{-2} intensity causes significant burn marks. In the case of red-to-blue TTA-UC, our data show that upconversion-mediated drug activation is possible at relatively low power without any tissue ablation.

Finally, the irradiation experiment was repeated with higher intensity red light (300 mW, 4.2 W.cm^{-2} intensity) and the absorption spectrum was measured every 30 min (Figure 8.13d and e). The evolution of the absorption band of **9**$^{2+}$ between 460 and 600 nm reached completion after approximately 2 h of irradiation, which indicates that a higher irradiation intensity indeed leads to more activation. Again, no visible signs of irradiation damage of the tissue were observed. In conclusion, the data show that activation of complex **6**$^{2+}$ by red light in combination with red-to-blue TTA-UC could be realized through a 7 mm thick slice of pork fillet. Furthermore, the results demonstrate that TTA-UC mediated photoactivation of photo-pharmacological compounds such as Ru-compounds is a promising and feasible strategy that may lead to treatment of tumors without tissue ablation.

8.2.9 Testing *in vitro* toxicity of M1-3-6 liposomes in hypoxic conditions with red light irradiation

The photocytotoxicity under high power red light was evaluated of **M1-3-6** liposomes that contained TTA-UC dyes **1** and **3**, and Ru-complex **6**$^{2+}$ in A549 and MRC5 cells. The same experimental protocol was used as in Section 8.2.6, but with a few important adaptations. The liposomes were tested only at 0.1 mM concentration, because **M1-3** liposomes were not toxic at this concentration. To enhance the amount of upconverted photons, (i) the cells were co-treated with 5 mM L-Asc and GSH, (ii) the irradiation was performed with a much higher light intensity and dose than before (1.1 W.cm^{-2} intensity, 5 min irradiation, 320 J.cm^{-2} dose), (iii) the irradiation was performed under hypoxic conditions (1% O_2), and (iv) another plate design was used (Figure 8.18). As controls, liposomes were used that contained only the TTA-UC dyes (**M1-3**), and liposomes deprived of photosensitizer (**M3-6**). As always, all experiments were also performed without irradiation in the dark. In order to reach the higher light intensity, instead of using LED arrays, which cannot reach such intensities, a PDT laser with collimating lens was fitted underneath the plate. As a consequence, not all wells could be irradiated at the same time,

the irradiation time per well needed to be short, the total irradiation time was higher (2 h in total), and the statistical error on the data was higher.

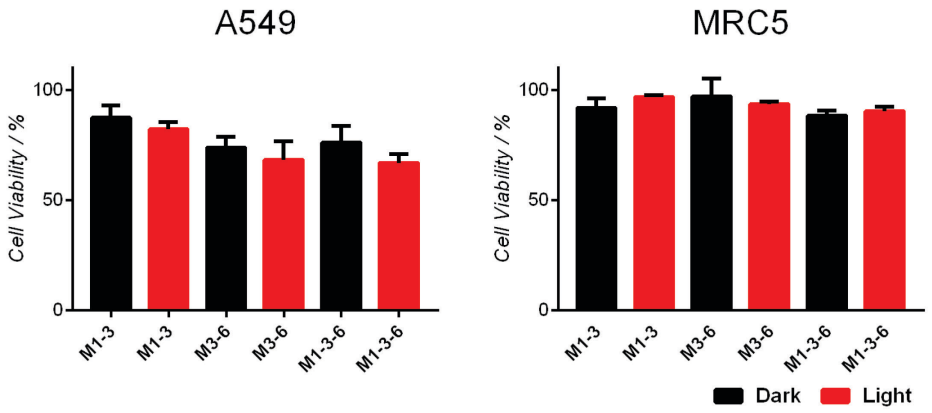

*Figure 8.14. Cell viability of A549 (left) and MRC5 cells (right) that were treated with **M1-3**, **M3-6**, and **M1-3-6** liposomes ([DMPC] = 0.1 mM), co-treated with 5 mM L-Asc and GSH, and irradiated with 1.1 W.cm^{-2} 630 nm light for 5 min (320 J.cm^{-2}) at 1% O_2 (red) or left in the dark under the same conditions (black). Error bars represent standard deviation of three individual wells. The experiment was conducted once.*

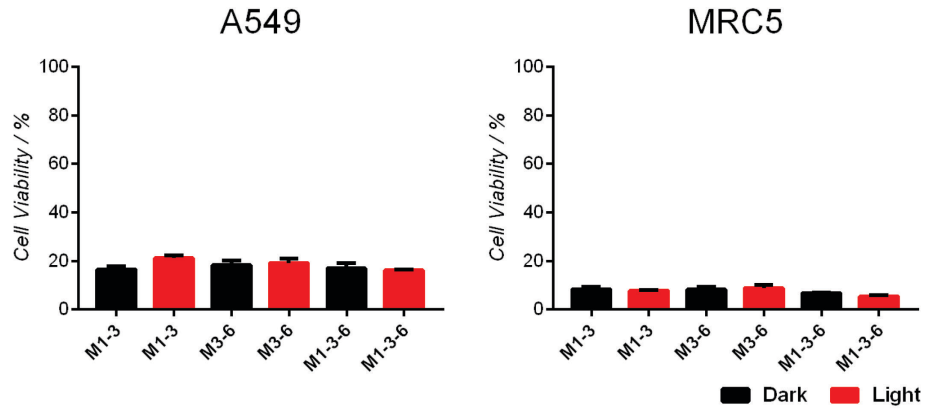

*Figure 8.15. Cell viability of A549 (left) and MRC5 cells (right) that were treated with **M1-3**, **M3-6**, and **M1-3-6** liposomes ([DMPC] = 0.1 mM), co-treated with 5 mM L-Asc and GSH, and irradiated with 1.1 W.cm^{-2} 630 nm light for 5 min (320 J.cm^{-2}) at 1% O_2 (red) or left in the dark under the same conditions (black). In this experiment, the medium was not refreshed either before or after irradiation, so that the liposomes and anti-oxidants were present during the last 72 h of the treatment. Error bars represent standard deviation of three individual wells. The experiment was conducted once.*

In Figure 8.14, the cell viability of A549 and MRC5 cells is reported after treatment with **M1-3**, **M3-6**, and **M1-3-6** liposomes that were irradiated or left in the dark. For both cell lines, **M1-3** liposomes were not found to be significantly toxic in dark and light conditions, consistent with the results discussed in Section 8.2.4. In dark conditions, **M3-6** liposomes were found to be more toxic in A549 cells than **M1-3** liposomes, but were not toxic in MRC5 cells. Red-light irradiation did not significantly influence the toxicity. Finally, in dark conditions, **M1-3-6** liposomes were found to be equally toxic as **M3-6** liposomes in both cell lines. Again, irradiation did not significantly influence the toxicity. To summarize: MRC5 cells were unaffected by any treatment, while a mild toxicity regardless of irradiation was observed for **M3-6** or **M1-3-6** liposomes in A549 cells. Because the toxicity of **M3-6** and **M1-3-6** liposomes is equal, the toxicity is most probably caused by the dark toxicity of compound $\mathbf{6}^{2+}$ (see Section 8.2.6). Furthermore, the result that light irradiation did not change the toxicity of **M1-3-6** liposomes in A549 cells was expected based on the results of **M6** liposomes (Section 8.2.6), which showed that the conversion of $\mathbf{6}^{2+}$ to $\mathbf{9}^{2+}$ upon irradiation does not cause more toxicity in A549 cells. In contrast, blue light irradiation of **M6** in MRC5 cells caused a decrease in cell viability at 0.1 mM from 82% in the dark to 55% in light conditions (Figure 8.10). Thus, the fact that **M1-3-6** liposomes are not toxic in MRC5 cells upon 5 min red light irradiation may indicate that upconversion was not effective in triggering the photodissociation reaction of $\mathbf{6}^{2+}$ to $\mathbf{9}^{2+}$. Most probably, 5 min of red light irradiation is simply not enough to release enough toxic $\mathbf{9}^{2+}$. For instance, in the preceding experiments discussed in Section 8.2.7, conducted in ideal, deoxygenated conditions, 30 – 60 min was needed to convert all $\mathbf{6}^{2+}$ to $\mathbf{9}^{2+}$ at similar light intensity. Furthermore, it is uncertain to what extent the toxicity of $\mathbf{9}^{2+}$ is affected by the presence of L-Asc and GSH, as it is known for example that GSH greatly decreases the toxicity of metallodrugs such as cisplatin.[19]

As a final experiment the cell treatment was repeated without removing the liposomes and anti-oxidants from the cell medium; the liposomes and anti-oxidants were present during the last 72 h of the photocytotoxicity assay. During irradiation stable upconversion emission was detected in the whole well volume when the plate was viewed with red-light blocking laser goggles. The cell viability of the A549 and MRC5 cells after treatment is plotted in Figure 8.15. Apart from the great decrease in viability in all wells, attributed to the continuous presence of liposomes and anti-oxidants, only minor

differences in cytotoxicity were observed in A549 cells that had been treated with **M1-3**, **M3-6**, or **M1-3-6** liposomes. Thus, under these conditions the toxicity of red-light irradiated **M1-3-6** liposomes is not substantial. Much further work is necessary to elucidate the conditions at which the activation of Ru-prodrugs using TTA-UC causes significant photocytotoxicity in cancer cells. For instance, Ru-complexes with a better photo-index are needed so that the upconversion strategy may be better tested *in vitro*. Also, longer irradiation times are required to release enough Ru-complex to induce a potentially toxic effect.

8.3 Conclusion

In this chapter, the biological applicability of three liposome systems was addressed: upconverting liposomes (System A), Ru-prodrug doped liposomes (System B), and liposomes doped with both upconverting dyes and Ru-prodrugs (System C). First of all, it was found that the biocompatible anti-oxidants L-Asc and GSH at biologically relevant concentrations greatly enhanced TTA-UC for **L1-2** liposomes in solution and in **M1-3** liposomes in cancer cells (System A). Then, it was established that **M1-3** liposomes are not (photo)cytotoxic in A549, MCF7, and MRC5 cell lines in the dark in and in red-light irradiated conditions; no PDT effect was observed, even at relatively high red light dose. Photocytotoxicity studies with Ru-prodrug functionalized liposomes **M5** and **M6** (System B) showed that both liposome formulations were considerably toxic in the dark, and that blue light irradiation enhanced their toxicity only slightly. Furthermore, it was demonstrated that photoactivation of Ru-prodrugs in liposomes mediated by red-to-blue TTA-UC (System C) could be obtained in air by adding biologically relevant concentrations of L-Asc and GSH. The same reaction could be triggered when a thick slice of pork fillet was placed between the laser and the sample, which illustrates the practical applicability of upconverting liposomes. Finally, the photocytotoxicity of **M1-3-6** liposomes was investigated under high power red light irradiation. Unfortunately, no significant cytotoxic effect was observed, which may be due to a low overall activation efficiency or to the poor cytotoxicity of the activated Ru-drug $\mathbf{9}^{2+}$. Overall, our results pave the way for photoactivation of Ru-complexes by TTA-UC *in vitro*, and give important insights in what requirements need to be fulfilled in order to make the activation-by-upconversion strategy perform well in a biological context: important optimization parameters that need to be considered include nanoparticle design, excitation wavelength and intensity, local oxygen

concentration and presence of anti-oxidants, TTA-UC emission stability, light dose, tissue thickness, and photo-index of Ru-prodrugs.

8.4 Experimental section

8.4.1 General

Palladium tetraphenyltetrabenzoporphyrin (**1**) was purchased from Frontier Scientific, Inc. (Logan, Utah, USA). Perylene (**2**) was purchased from Sigma-Aldrich Chemie BV (Zwijndrecht, The Netherlands). The synthesis of 2,5,8,11-tetra(*tert*-butyl)perylene (compound **3**) is described in Chapter 9. The synthesis of **4**$(PF_6)_2$ is described in section 3.4.2. The synthesis of [Ru(tpy)(bpy)(Cl)](Cl) is described elsewhere.[20] Compounds **5**$(PF_6)_2$ was synthesized by Lucien Lameijer. Compounds **10**, **11**, **12**, **6**$(PF_6)_2$, and **7**$(PF_6)_2$ were synthesized by Michael Meijer. Sodium N-(carbonyl-methoxypolyethylene glycol-2000)-1,2-distearoyl-sn-glycero-3-phospho ethanolamine (DSPE-mPEG-2000), 1,2-dilauroyl-sn-glycero-3-phosphocholine (DLPC), and 1,2-dimyristoyl-sn-glycero-3-phosphocholine (DMPC) were purchased from Lipoid GmbH (Ludwigshafen, Germany) and stored at −18 °C. Dulbecco's phosphate buffered saline (PBS) was purchased from Sigma Aldrich and had a formulation of 8 $g.L^{-1}$ NaCl, 0.2 $g.L^{-1}$ KCl, 0.2 $g.L^{-1}$ KH_2PO_4, and 1.15 $g.L^{-1}$ K_2HPO_4 with a *pH* of 7.1 – 7.5. Anti-oxidant supplemented PBS was prepared by dissolving L-ascorbic acid and/or glutathione in PBS and neutralizing with sodium hydroxide to *pH* 7.0 − 7.6. Other chemicals were purchased from major chemical suppliers and used as received. Images and data were processed with Fiji ImageJ, Origin Pro, and Microsoft Excel software. Emission and absorption spectroscopy, and photodissociation experiments using red light were performed in experimental setups reported in other chapters (see Sections 4.4.5 and 6.4.4). Photodissociation experiments using blue light were recorded in a Cary 50 Varian spectrometer equipped with a Cary Single Cell Peltier for temperature control.

8.4.2 Synthesis of 5$(PF_6)_2$

To a suspension of [Ru(tpy)(bpy)Cl]Cl (202 mg, 0.360 mmol) in acetone/H_2O (9:1, 40 mL) were added dodecyl(methyl)sulfide (1.17 g, 5.41 mmol) and $AgPF_6$ (200 mg, 0.791 mmol). This mixture was heated at 55° C for 24 hours under argon, after which the solvent was removed by rotary evaporation. The residue was dissolved in a minimal amount of acetone and precipitated by the addition of Et_2O. Collection by filtration and washing with Et_2O (3×) afforded [Ru(tpy)(bpy)(dodecyl(methyl)sulfide)]$(PF_6)_2$ (compound **5**$(PF_6)_2$) as a red-brown precipitate (250 mg, 0.251 mmol, 70%). TLC: R_f = 0.64 (100/10/2 acetone/water/sat. KPF_6). ^{1}H NMR (400 MHz, CD_3OD) δ = 9.79 (d, J = 6.3 Hz, 1H, H_a), 8.82 (d, J = 7.7 Hz, 1H, H_A), 8.78 (d, J = 8.2 Hz, 2H, H_D+H_G), 8.63 (d, J = 8.0 Hz, 2H, H_E+H_H), 8.59 (d, J = 7.0 Hz, 1H, H_K), 8.40 (t, J = 8.0 Hz, 2H, H_B+H_F), 8.15 – 8.00 (m, 4H, H_I+H_J+H_b)), 7.92 (t, J = 7.8 Hz, 1H, H_c), 7.81 (d, J = 6.4 Hz, 2H, H_d+H_e), 7.50 – 7.39 (m, 2H, H_C+H_f), 7.28 (d, J = 5.0 Hz, 1H, H_h), 7.27 – 7.18 (m, 1H, H_g), 1.65 (dd, J = 8.4, 6.5 Hz, 2H, H_2), 1.36 (s, 3H, H_1), 1.34 – 1.11 (m, 16H, H_3 – H_{10}), 1.09 – 1.00 (m, 4H, H_{11}+H_{12}), 0.93 – 0.84 (m, 3H, H_{13}). ^{13}C NMR (100 MHz, CD_3OD) δ = 158.1 (Quat. Arom.), 157.4 (Quat. Arom.), 156.7 (Quat. Arom.), 153.0 (C_d+C_e), 151.83 (Quat. Arom.), 151.7 (C_a), 151.6 (Quat. Arom.), 149.4 (C_h), 138.8 (C_I+C_J), 138.2 (C_c), 138.0 (C_B), 136.9 (C_F), 128.4 (C_C+C_f), 127.8 (C_b), 127.1 (C_h), 124.9 (C_E+C_H), 124.6 (C_K), 124.1 (C_D+C_G) 123.8 (C_A), 33.5 (C_2), 31.7 (C_{10}), 29.4 (C_9), 29.3 (C_8), 29.1 (C_7), 28.6 (C_6), 28.0 (C_5), 26.4 (C_4), 22.4 (C_3), 19.0 (C_2), 13.2 (C_1+C_{13}). ESI-MS m/z exp. (calcd.): 261.7 (261.5, $[M\text{-}2PF_6\text{-}H_2O\text{+}MeOH]^{2+}$); 353.5 (353.6, $[M\text{-}2PF_6]^{2+}$); 522.0 (522.1, $[M\text{-}2PF_6\text{-}H_2O\text{+}MeO]^{+}$);

852.2 (852.2, $[M\text{-}PF_6]^+$). UV-Vis: λ_{max} in H_2O: 452 nm (ε = 6300 $M^{-1}.cm^{-1}$). Photosubstitution quantum yield = 0.0070 in H_2O (λ_{exc} = 452 nm), as determined with a literature procedure.[21]

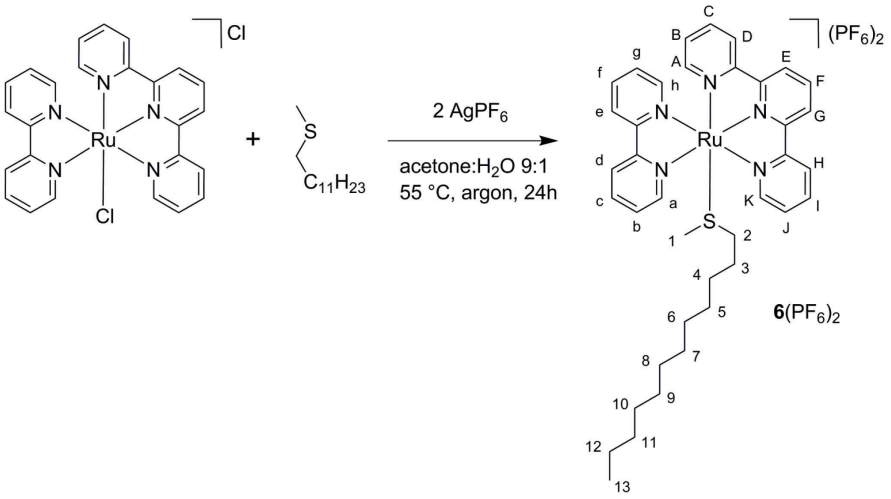

*Scheme 8.1. Synthesis of compound **5**$(PF_6)_2$ from [Ru(tpy)(bpy)Cl]Cl and dodecyl(methyl)sulfide.*

8.4.3 Synthesis of 1,3-bis(methylthio)-2-dodecyloxypropane – compound 10

To a stirred suspension of NaH (222 mg, 5.55 mmol) in dry and deoxygenated THF (5 mL) under Ar atmosphere was added 1,3-bis(methylthio)-2-propanol (0.25 mL, 1.85 mmol). The mixture was stirred at RT for 10 min, after which 1-bromododecane (0.5 mL, 2.13 mmol) was added dropwise, resulting in a light-brown suspension. The reaction mixture was heated to reflux for 20 h. Hereafter, the mixture was concentrated to 1 – 2 mL, Et_2O (40 mL) was added, and the resulting mixture was washed with brine (40 mL), 1 M aq. NH_4Cl (2 × 40 mL) and brine (40 mL). The organic layer was dried with $MgSO_4$ and the solvent was removed by rotary evaporation. After column chromatography (SiO_2, petroleum ether 40-60: DCM (2:1) to neat DCM) the title compound was obtained as a light-yellow oil (250 mg, 0.78 mmol, 42%). TLC: R_f = 0.9 (DCM). ^1H NMR (300 MHz, δ in $CDCl_3$): 3.58 (p, J = 5.8 Hz, 1H, H3), 3.51 (t, J = 6.6 Hz, 2H, H1'), 2.74 (ddd, J = 18.9, 13.6, 5.8 Hz, 4H, H2+H4), 2.16 (s, 6H, H1+H5), 1.65 – 1.51 (m, 2H, H2'), 1.42 – 1.18 (m, 18H, H3'-H11'), 0.88 (t, J = 6.5 Hz, 3H, H12'); ^{13}C NMR (75 MHz, δ in $CDCl_3$): 79.3, 70.3, 37.7, 32.1, 30.2, 29.8, 29.8, 29.8, 29.7, 29.6, 29.5, 26.3, 22.8, 16.9, 14.3; ESI-MS m/z exp. (calcd.): 135.1 (135.0, $[M\text{-}C_{12}H_{25}O]^+$), 208.0 (208.2, $[C_{12}H_{25}O+Na]^+$), 321.2 (321.2, $[M+H]^+$).

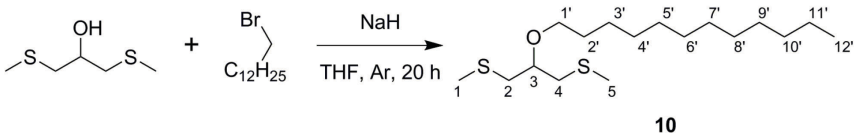

*Scheme 8.2. Synthesis of compound **10** from 1,3-bis(methylthio)-2-propanol and 1-bromododecane.*

8.4.4 Synthesis of $6(PF_6)_2$

A mixture of compound **10** (66 mg, 0.206 mmol) and *cis-Λ/Δ*-$[Ru(bpy)_2Cl_2]$ (50 mg, 0.103 mmol) under Ar atmosphere was dissolved in a 1:1 mixture of EtOH and H_2O (10 mL) and heated to reflux in the dark for 20 h. Hereafter, the reaction mixture was cooled to room

temperature, and the solvent was removed *in vacuo.* The reaction mixture was poured onto 30 mL of sat. aq. KPF_6, extracted with DCM (4 × 20 mL), and concentrated by rotary evaporation. Removal of the excess ligand was done by centrifugal washing with diethyl ether (2 × 12 mL, 2800 g). *cis-Λ/Δ*-[Ru(bpy)$_2$(**10**)](PF6)$_2$ (compound **6**$(PF_6)_2$) was obtained as an orange powder in 45% yield (47 mg, 0.046 mmol). ^{1}H NMR (400 MHz, δ in CD_3CN): 9.62 (d, J = 5.3 Hz, 1H, H_H), 9.17 (d, J = 5.3 Hz, 1H, H_h), 8.52 (t, J = 8.7 Hz, 2H, H_e+H_E), 8.38 (dd, J = 8.2, 2.8 Hz, 2H, H_d+H_D), 8.33 – 8.24 (m, 2H, H_f+H_F), 8.03 – 7.96 (m, 2H, H_c+H_C), 7.93 – 7.85 (m, 2H, H_g+H_G), 7.49 (d, J = 5.1 Hz, 1H, H_A), 7.43 (d, J = 5.1 Hz, 1H, H_a), 7.36 – 7.26 (m, 2H, H_b+H_B), 4.37 (s, 1H, H3), 3.67 (dt, J = 9.2, 6.5 Hz, 1H, H1'), 3.49 (dt, J = 9.2, 6.5 Hz, 1H, H1'), 3.20 (dd, J = 13.2, 6.2 Hz, 1H, H4), 3.12 (dd, J = 13.9, 2.7 Hz, 1H, H2), 2.95 (s, 1H, H2), 2.61 (dd, J = 13.1, 1.6 Hz, 1H, H4), 1.66 – 1.54 (m, 2H, H2'), 1.43 (s, 3H, H1), 1.40 – 1.21 (m, 18H, H3'-11'), 1.08 (s, 3H, H5), 0.88 (d, J = 6.8 Hz, 3H, H12'); ^{13}C NMR (100 MHz, δ in CD_3CN): 158.6 (C_q), 158.5 (C_q), 157.3 (C_q), 157.2 (C_q), 154.6 (C_h), 153.9 (C_H), 152.2 (C_a), 151.9 (C_A), 139.8 (C_c+C_C+C_f+C_F), 129.7 (C_g), 128.7 (C_b+C_B), 128.6 (C_G), 125.9 (C_e), 125.8 (C_E), 125.2 (C_d), 125.1 (C_D), 74.2 (C3), 70.4 (C1'), 38.0 (C4), 37.2 (C2), 32.6, 30.5, 30.3, 30.3, 30.0, 26.8, 23.4, 20.9 (all C2'-11'), 18.5 (C1), 16.0 (C5), 14.4 (C12'); HR-MS m/z exp. (calcd.): 367.1310 (367.1312, $[M\text{-}2PF_6]^{2+}$); UV-Vis: λ_{max} (ε in $L.mol^{-1}.cm^{-1}$) in CH_3CN: 415 nm (6172); Elemental analysis for $C_{37}H_{52}F_{12}N_4OP_2RuS_2$: (calcd.): C, 43.40; H, 5.12; N, 5.47; (exp.): C, 43.38; H, 5.15; N, 5.49.

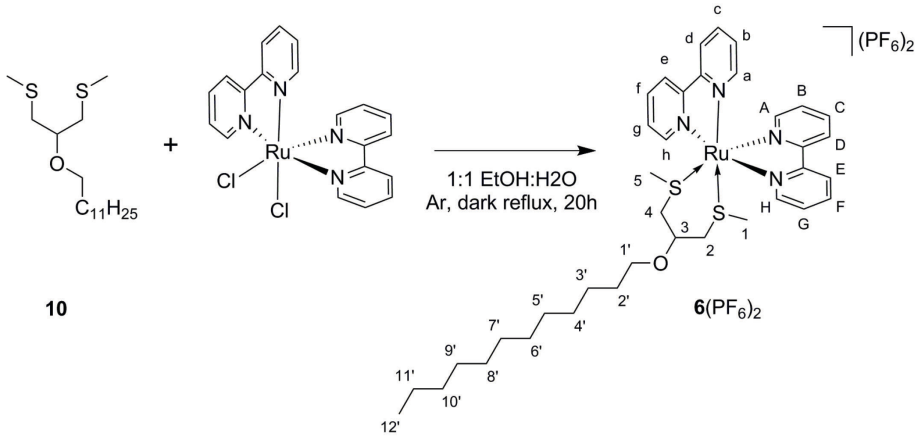

Scheme 8.3. Synthesis of ***6****$(PF_6)_2$ from compound* ***10*** *and cis-Λ/Δ-[Ru(bpy)$_2$Cl$_2$].*

8.4.5 Synthesis of 2,9-dimethyl-1,10-phenanthroline-5,6-dione – compound 11

According to literature procedure.[22] **11** was obtained as ocher yellow needles in 59% yield (2.03 g, 8.53 mmol). ^{1}H NMR (300 MHz, δ in $CDCl_3$): 8.38 (d, J = 8.0 Hz, 2H, H4+H7), 7.42 (d, J = 8.0 Hz, 2H, H3+H8), 2.86 (s, 6H, H2+H9); Spectrum matches literature data.[22] ESI-MS m/z exp. (calcd.): 239.1 (239.1, $[M+H]^+$), 261.1 (261.1, $[M+Na]^+$).

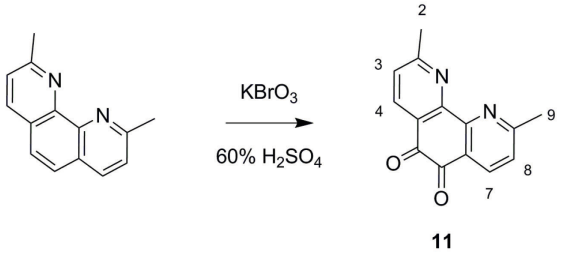

*Scheme 8.4. Synthesis of compound **11**.*

8.4.6 Synthesis of 5,6-bis(dodecyloxy)-2,9-dimethyl-1,10-phenanthroline – compound 12

Compound **11** (500 mg, 2.10 mmol) was dissolved in a 1:1 mixture of H_2O and THF (20 mL), and placed under Ar atmosphere, followed by the addition of tetrabutylammonium bromide (451 mg, 1.40 mmol), sodium dithionite (2.19 g, 12.6 mmol) and 1-bromododecane (1.66 mL, 6.93 mmol). To the resulting yellow suspension was slowly added a solution of KOH (1.77 g, 31.5 mmol) in H_2O (10 mL), leading to a dark brown suspension. The reaction mixture was stirred at 40 °C for 3 days, during which the color lightened to yellow-brown. After dilution with H_2O (50 mL), the mixture was extracted with EtOAc (3 x 75 mL). The combined organic layers were washed with H_2O (100 mL), dried over $MgSO_4$ and the solvent was removed by rotary evaporation. Column chromatography (SiO_2, EtOAc) yielded the title compound in 59% yield as a beige powder (720 mg, 1.25 mmol). TLC: R_f = 0.8 (EtOAc). ^{1}H NMR (300 MHz, δ in $CDCl_3$): 8.45 (d, J = 8.4 Hz, 2H, H4+H7), 7.49 (d, J = 8.4 Hz, 2H, H3+H8), 4.21 (t, J = 6.7 Hz, 4H, H1'), 2.93 (s, 6H, H2+H9), 1.88 (p, J = 6.7 Hz, 4H, H2'), 1.61 – 1.48 (m, 4H, H3'), 1.45 – 1.20 (m, 32H, H4'-H11'), 0.88 (t, J = 6.9 Hz, 6H, H12'); ^{13}C NMR (75 MHz, δ in $CDCl_3$): 158.2, 141.9, 131.0, 124.4, 123.7, 74.1, 32.1, 30.6, 29.8, 29.8, 29.7, 29.5, 26.4, 25.7, 22.9, 14.3; HR-MS m/z exp. (calcd.): 577.4721 (577.4728, $[M+H]^+$).

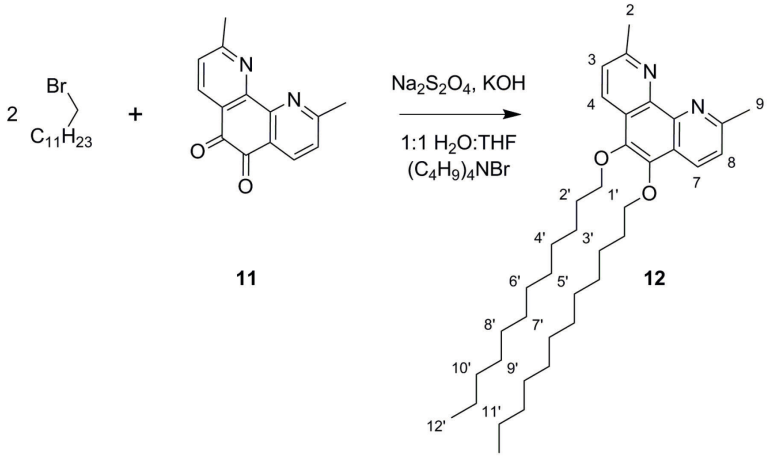

*Scheme 8.5. Synthesis of compound **12** from 1-bromododecane and compound **11**.*

8.4.7 Synthesis of 7$(PF_6)_2$

A mixture of **12** (100 mg, 0.172 mmol) and *cis-Λ/Δ*-[Ru(bpy)$_2$Cl$_2$] (100 mg, 0.206 mmol) was placed in a 25-mL Teflon-lined stainless steel reaction vessel. Ethylene glycol (8 mL) was added, and the closed vessel was heated to 200 °C for 6 h. The red solution obtained was poured onto

water (50 mL) and an orange precipitate was produced by adding sat. aq. KPF_6 (5 mL). After cooling the mixture to 4 °C, the precipitate was collected by filtration, washed with cold water and cold Et_2O, and purified by column chromatography (SiO_2, acetone to acetone:H_2O:sat. aq. KPF_6 (100:10:2)). Further purification using size exclusion chromatography (Sephadex LH20, acetone) yielded *cis-Λ/Δ*-[Ru(bpy)$_2$(**12**)]$(PF_6)_2$ (compound **7**$(PF_6)_2$) as a red powder (29 mg, 0.023 mmol, 13%). ^{1}H NMR (300 MHz, δ in CD_3CN): 8.63 (d, J = 8.5 Hz, 2H, H4+H7), 8.49 (d, J = 8.1 Hz, 2H, H_e), 8.43 (d, J = 8.1 Hz, 2H, H_d), 8.02 (td, J = 8.0, 1.5 Hz, 2H, H_f), 7.97 (td, J = 8.0, 1.5 Hz, 2H, H_c), 7.68 (d, J = 5.3 Hz, 2H, H_a), 7.61 (d, J = 5.1 Hz, 2H, H_h), 7.56 (d, J = 8.5 Hz, 2H, H3+H8), 7.27 (dd, J = 5.7, 1.0 Hz, 2H, H_g), 7.23 (dd, J = 5.7, 1.1 Hz, 2H, H_b), 4.38 – 4.18 (m, 4H, H1'), 1.91 – 1.83 (m, 10H, H2+H9+H2'), 1.54 (p, J = 7.1 Hz, 4H, H3'), 1.41 – 1.21 (m, 32H, H4'-H11'), 0.88 (t, J = 6.5 Hz, 6H, H12'); ^{13}C NMR (75 MHz, δ in CD_3CN): 166.6, 153.8 (C_h), 152.9 (C_a), 138.8 (C_c), 138.6 (C_f), 133.1 (C4+C7), 128.3 (C3+C8+C_b+C_g), 125.4 (C_d+C_e), 75.4 (C1'), 32.7 (C2'), 30.8, 30.4, 30.3, 30.1, 26.8 (all C3'-C10'), 26.0 (C2+C9), 23.4 (C11'), 14.4 (C12'); HR-MS m/z exp. (calcd.): 495.2534 (495.2539, $[M\text{-}2PF_6]^{2+}$); UV-Vis: λ_{max} (ε in L.mol^{-1}.cm^{-1}) in CH_3CN: 452 nm (13730); Elemental analysis for $C_{58}H_{76}F_{12}N_6O_2P_2Ru$: (calcd.): C, 54.41; H, 5.98; N, 6.56; (exp.): C, 54.94; H, 5.23; N, 6.58.

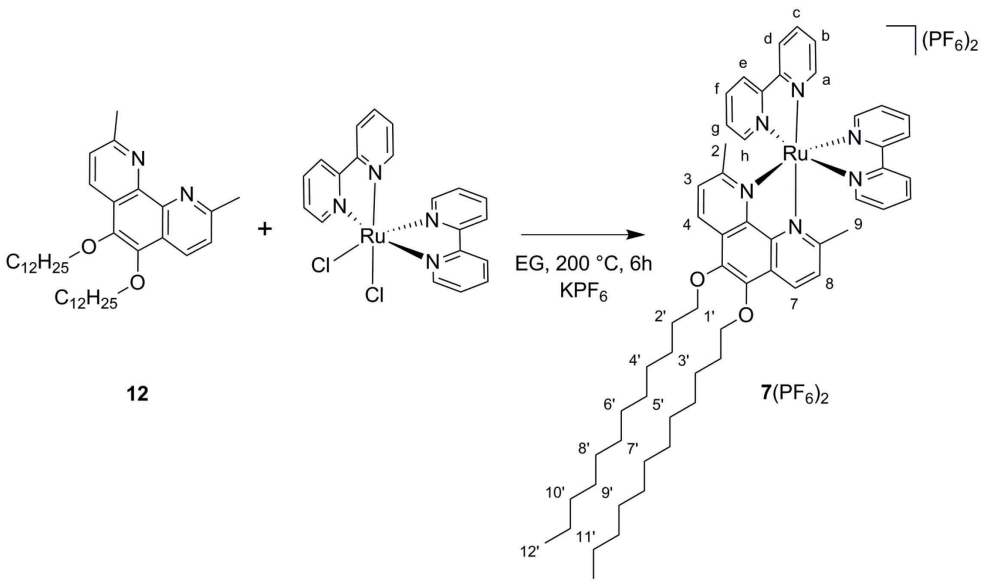

*Scheme 8.6. Synthesis of compound **7**$(PF_6)_2$ from cis-Λ/Δ-[Ru(bpy)$_2$Cl$_2$] and compound **12**.*

8.4.8 Liposome preparation

All liposome formulations were prepared by the classical hydration-extrusion method. As an example, the preparation of **M1-3-6** is described here. Aliquots of chloroform stock solutions containing the liposome constituents were added together in a flask to obtain a solution with 5.0 µmol DMPC, 0.20 µmol DSPE-mPEG-2000, 2.5 nmol **1**, 25 nmol **3**, and 0.20 µmol **6**$[PF_6]_2$. The organic solvent was removed by rotary evaporation and subsequently under high vacuum for at least 30 minutes to create a lipid film. 1.0 mL PBS buffer (with or without L-ascorbic acid and/or glutathione) was added and the lipid film was hydrated by 4 cycles of freezing the flask in liquid nitrogen and thawing in warm water (50 °C). The resulting dispersion was extruded through a Whatman Nuclepore 0.2 µm polycarbonate filter at 40-50 °C at least 11 times using a mini-

extruder from Avanti Polar Lipids, Inc. (Alabaster, Alabama, USA). The number of extrusions was always odd to prevent any unextruded material ending up in the final liposome sample. The extrusion filter remained practically colorless after extrusion, suggesting near-complete inclusion of the chromophoric compounds in the lipid bilayer. Liposomes were stored in the dark at 4 °C and used within 7 days. The average hydrodynamic liposome size and polydispersity index (PDI) were measured with a Malvern Instruments Zetasizer Nano-S machine, operating with a wavelength of 632 nm. The size and PDI were typically 130 – 170 nm and 0.1, respectively.

8.4.9 Upconversion emission spectroscopy with L1-2 liposomes and meat

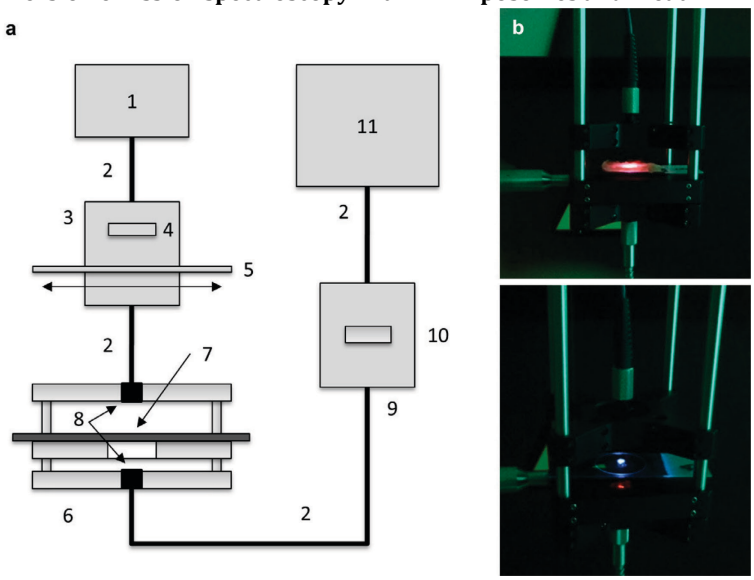

Figure 8.16. Experimental setup used for spectroscopy through meat. a) Schematic representation of the setup: 630 nm laser (1); optical fibers (2); filter holder (3) for 630 nm band pass filter (4) and variable neutral density filter (5); cage system (6) with two oppositely facing cage plates, both fitted with a collimating lens (8), and a central sample-holding plate; microscopy slide holding the liposome gel and meat on top (7); filter holder (9) for a 630 nm notch filter (10) for blocking the excitation source; spectrometer (11). b) Photographs of the cage system with the upconverting liposome gel only (bottom) and with 1 layer of pork fillet on top (top). Both photographs were taken with a 575 nm OD 4 short pass filter in front of the camera to block the excitation source.

L1-2 liposomes were prepared according to Section 8.4.8 ([DLPC] = 20.0 mM). To prepare a liposome hydrogel and to allow upconversion in air, this solution was heated to 55 °C and 1:1 v/v mixed with a solution at 55 °C containing 1 wt.% agarose, 10 mM sodium L-ascorbate and 10 mM sodium glutathionate (*pH* 7.3). 20 µL of this mixture was pipetted with a warm pipet on a warm 1 mm thick microscopy slide (Menzel-Gläser Superfrost, 76 x 26 mm) and immediately covered with a round 25 mm diameter microscopy coverslip (VWR, thickness no. 1). Upon cooling to room temperature, this procedure produced a thin gel slice with ~25 µm thickness. On top of the coverslips, thin slices of chicken breast fillet or pork fillet were layered (1 – 2 mm thick each, measured for each slice with a caliper) up to ~13 mm thick. The entire sample construct was allowed to reach room temperature (20 °C) before measurement in a custom-build spectroscopy setup (Figure 8.16). A cage with an open sample space was constructed with

single collimating lenses (Avantes COL-UV/VIS) on both sides for excitation (from the top) and detection (from the bottom) connected with FC-UVxxx-2 (xxx = 400, 600) optical fibers (Avantes). The excitation lens was connected to a clinical grade Diomed 630 nm PDT laser set to 30 mW (3 mm beam, 0.42 $W.cm^{-2}$) using a PM100 USB power meter and S310C detector (Thorlabs). Between the laser and the excitation lens, a filter holder was placed with a FB630-10 band pass filter and a NDL-25C-4 variable neutral density filter (Thorlabs). The detection lens was connected to a 2048L StarLine spectrometer (Avantes); between the spectrometer and detection lens, a filter holder with a NF-633 notch filter was placed. For each meat layer thickness, the spectrum was taken at 5 different sample locations, and the spectrum was averaged. Then, a new layer of meat was carefully placed on top and the measurements were repeated until a thickness of ~13 mm was achieved.

8.4.10 Photodissociation experiments with meat

For photodissociation experiments with **L1-3-6** liposomes and meat, the sample was prepared as described in Section 8.4.8 ([DLPC] = 10 mM). 400 µL sample was placed in a 2 mm thick cuvette and sandwiched between a 5 × 5 cm glass plate and a 5 × 5 cm slice of pork fillet (Albert Heijn; "AH Filetlapjes à la minute naturel"), 7 ± 0.5 mm thick. This meat-sample construct was placed in the same cage setup as described in Section 8.4.9, but the laser was now directly coupled to the excitation lens and the FB630-10 band pass filter was now placed directly between the excitation lens and the sample (see Figure 8.13). The detection lens and spectrometer were left out. To compare blue and light irradiation, the meat-sample construct was irradiated from the top with either 110 mW 450 nm or 630 nm laser light in a 3 mm collimated beam (1.6 $W.cm^{-2}$). Also, the experiment was repeated with 300 mW 630 nm light (4.2 $W.cm^{-2}$).

8.4.11 General cell culturing

A549 human lung carcinoma cells were cultured in 25 cm^2 flasks in 8 mL Dulbecco's Modified Eagle Medium with phenol red (DMEM; Sigma Life Science, USA), supplemented with 8.2% v/v fetal calf serum (FCS; Hyclone), 200 $mg.L^{-1}$ penicillin and streptomycin (P/S; Duchefa), and 1.8 mM glutamine-S (GM; Gibco, USA), under standard culturing conditions (humidified, 37 °C atmosphere containing 7.0% CO_2). The cells were split approximately once per week upon reaching 70 − 80% confluency, using seeding densities of 2 × 10^5 cells, and the medium was refreshed once per week. Cells were passaged for 4 − 8 weeks.

8.4.12 Live cell imaging with M1-3 liposomes - preparation

After cell splitting, the cells were suspended in OptiMEM (Life Technologies, USA), supplemented with 2.5% FCS, 200 mg/L P/S, and 1.8 mM GM at 3 × 10^5 cells per mL. 100 µL of this suspension was placed in a droplet on round 25 mm diameter microscopy coverslips (VWR, thickness no. 1) in a 6-well plate. After 5 min of sedimentation, 3 mL OptiMEM was carefully added to each well, and the cells were incubated for 24 h. Meanwhile, **M1-3** liposome samples were prepared as before ([DMPC] = 2.5 mM, 2 mL volume). Optionally, this solution contained 5 mM sodium L-ascorbate and 5 mM sodium glutathionate. The solution was sterilized with a 0.2 µm filter and from this a 3:5 v/v liposomes/Opti-MEM solution was prepared ([DMPC] = 1 mM). 3 mL of this solution was added to the desired wells, and the cells were incubated for 24 h. Then, the cells were washed once with PBS, and resupplied with 1 mL Opti-MEM before imaging. Optionally, the cells were incubated with 50 nM LysoTracker Red DND-99 in Opti-MEM for 30 min, after which the cells were washed once with PBS, and resupplied with 1 mL Opti-

MEM before imaging. Finally, the coverslips were transferred to a custom-made sample holder for round 25 mm coverslips, and supplied with 500 µL Opti-MEM.

8.4.13 Live cell imaging with M1-3 liposomes - microscopy

Bright field and (upconversion) emission imaging was performed with a customized Zeiss Axiovert S100 Inverted Microscope setup, fitted with a Zeiss 100× Plan Apochromat 1.4 NA oil objective, and an Orca Flash 4.0 V2 sCMOS camera from Hamamatsu, which together produced 4.2 megapixel images with pixel size of 69 nm. The typical camera exposure time was 1000 ms. Samples were loaded in a temperature and atmosphere controlled stage-top mini-incubator (Tokai Hit, Japan) set at 37 °C with 1% O_2 and 7% CO_2 in which samples were incubated for 30 min before imaging. For direct excitation and fluorescence imaging of **2**, a CrystaLaser DL-405-050 405 nm solid state laser was used, combined with a ZT405/514/561rpc dichroic beam splitter (Chroma Technology Corporation) and ZET442/514/568m emission filter (Chroma Technology Corporation). The output power of the 405 nm laser at the sample was typically 75 µW (60 µm spot diameter, intensity 2.7 W.cm^{-2}). For upconversion emission microscopy, a Power Technology 1Q1A30(639-35B)G3 639 nm diode laser was used as excitation source, combined with a Chroma ZT405/532/635rpc dichroic beam splitter. To block everything except upconversion emission, a 575 nm short pass filter (Edmund Optics, part no. #84-709) was placed between the sample and the camera, resulting in OD > 5 at 639 nm and 800 nm (*i.e.* the excitation source and the phosphorescence of **1** were completely blocked). The output power of the 639 nm laser at the sample was typically 1.0 mW (70 µm spot diameter, intensity 26 W.cm^{-2}). All laser beam spots had a Gaussian intensity profile; spot diameters are reported as Full Width at Half Maximum (FWHM) values.

8.4.14 Photocytotoxicity assay of liposomes with red and blue light

The phototoxicity of upconverting liposomes and liposomes doped with Ru-complexes was determined according to a photocytotoxicity protocol that was recently developed in our group.[10] MCF7, A549, or MRC5 cells were seeded in the central 60 wells of a 96 well plate at 8 K, 5 K, and 6 K cells respectively in 100 µL Opti-MEM. 100 µL Opti-MEM was added to the outer wells. The plate was incubated for 24 h. Meanwhile, liposomes were prepared as before ([DMPC] = 5.0 mM) and sterilized by extruding through a 0.2 µm filter. This procedure did not change the DLS values of the liposomes. The sterilized solution was used to prepare a dilution series of liposomes in 8-chamber reservoirs, and 100 µL of each diluted mixture was added to the wells according to the plate-design, see Figure 8.18a. The outer wells and control wells were mock-treated with 100 µL Opti-MEM only. The plates were incubated for 24 h, after which the cells were washed once with 200 µL Opti-MEM and resupplied with 200 µL Opti-MEM. The well-plate was placed in a temperature and atmosphere controlled stage-top mini-incubator (Tokai Hit, Japan) set at 37 °C, 20% O_2, and 7% CO_2 in which samples were incubated for 10 min before irradiation. Then, the plate was irradiated with either 15 min of 628 nm light (23.0 ± 1.5 mW.cm^{-2} intensity, 20.7 J.cm^{-2} dose) or 10 min of 454 nm light (7.0 ± 0.8 mW.cm^{-2} intensity, 4.2 J.cm^{-2} dose) using a custom-build array of 96 LED lights that fitted exactly on top of the mini-incubator, which have been characterized by our group recently.[10] The irradiation intensities were determined with a custom build spectroscopy setup, detailed in Section 8.4.15. Control plates were treated in the same way, but not irradiated. After irradiation, the plate was incubated for 48 h at 37 °C, 7% CO_2 and 20% O_2. Then, the cells were fixed by adding 100 µL 10% w/w trichloroacetic acid (TCA) in H_2O to each well and the plate was placed in a refrigerator at 4 °C for 60 h. The TCA was removed by rinsing the plate gently with H_2O five

times and the plate was dried overnight. Then, the inner 60 wells of the plate were stained with 100 µL sulforhodamine B (SRB, 0.6 w% in 1 v% acetic acid) for 30 min, after which the plate was washed five times in 1 v% acetic acid. Once the plate was dry (± 3 h), the SRB stain was dissolved in 200 µL 10 mM tris-base solution and the plate was placed on an orbital shaker for 30 min. Finally, the absorbance at 510 nm was measured with a plate reader (Tecan Infinite M1000 Pro) and the absorbance was converted to relative cell-viabilities using Microsoft Excel 2010 and GraphPad Prism 7 software. In case of **M1-3**, **M1**, and **M3** liposomes, the experiment was performed three times (three biological replicates); in case of **M5** and **M6**, the experiment was performed twice (two biological replicates).

8.4.15 Characterization of red and blue LED arrays in mini-incubator irradiation setup

The light power density of the LED arrays was measured using a custom-built spectroscopy setup consisting of an integrating sphere, which was positioned underneath the 96-well plate to simulate the irradiation conditions during cell experiments (Figure 8.17). The integrating sphere was mounted in a custom-made holder that mimicked the height of the mini-incubator while allowing the integrating sphere to be aligned exactly with a single 6 mm diameter well of a 96-well plate. On top of the holder, the lid of the mini-incubator was positioned, and on top of that, the LED array just like during cell irradiation. The integrating sphere position was diagonally adjustable over ten wells in order to individually measure a representative set of wells (B2, C3, C7, D4, D8, E5, E9, F6, F10, and G11). The integrating sphere was connected via an optical fiber to an Avantes CCD spectrometer, which were together spectrally calibrated just before measurement using a NIST-traceable calibration lamp (Avantes) to report the spectrum in spectral irradiance units ($\mu W.cm^{-2}.nm^{-1}$), where the surface here refers to that of the aperture of the integrating sphere. The light averaged intensity at the bottom of each well in $mW.cm^{-2}$ was then determined by spectrally integrating the spectrum for each well with OriginPro software and averaging these values over the different wells. Analysis of the spectrum also provided the intensity maximum and full-width-half-maximum (FWHM) bandwidth of each LED array. For the 454 nm LED array had a FWHM of 23 nm and an intensity of 7.0 ± 0.8 $mW.cm^{-2}$. The 628 nm LED array had a FWHM of 19 nm and an intensity of 23.0 ± 1.5 $mW.cm^{-2}$.

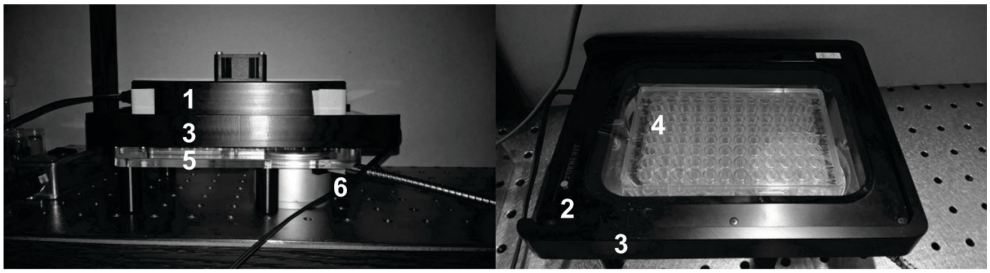

Figure 8.17. Photographs of the setup used for characterization of LED arrays, consisting of (from top to bottom) 96-LED array (1), mini-incubator lid (2), mini-incubator mimicking plate holder (3), 96-well plate (4), bottom of the plate holder (5), and integrating sphere fitting directly underneath the 96-well plate (6).

8.4.16 Photocytotoxicity assay of liposomes with high intensity red light

For photocytotoxicity assays using high intensity red light, a different procedure was followed; the differences are reported here. Instead of using all 60 central wells of a 96 well plate, only 24

of them were used according to the plate design in Figure 8.18b. Wells between the test-wells were intentionally left empty to avoid unintentional irradiation of neighboring wells. For this experiment, the diluted liposome solution (0.20 mM DMPC in Opti-MEM) was mixed 1:1 v/v with 10 mM sodium L-ascorbate and sodium glutathionate in PBS to make a 100 µM DMPC and 5 mM anti-oxidant solution. Additionally, the experiment was performed under hypoxic conditions by adjusting the O_2 level in the mini-incubator to 1%. Single wells were irradiated for 5 min with a 630 nm Diomed 630 PDT laser, fiber-coupled with a 600 µm fiber (Avantes) to a collimating lens (Omicron Laserprodukte GmbH, DE) fitted underneath the well plate (Figure 8.19). Together, these produced a 6 mm collimated beam (300 mW power, 1.1 $W.cm^{-2}$ intensity, 320 $J.cm^{-2}$ dose for 5 min irradiation) that illuminated an entire well surface area exactly. In these experiments, the well plate was moved every 5 min with an automated stage (MLS203-1, Thorlabs) so that each well was irradiated consecutively (2 h total irradiation time). This experiment was performed only once.

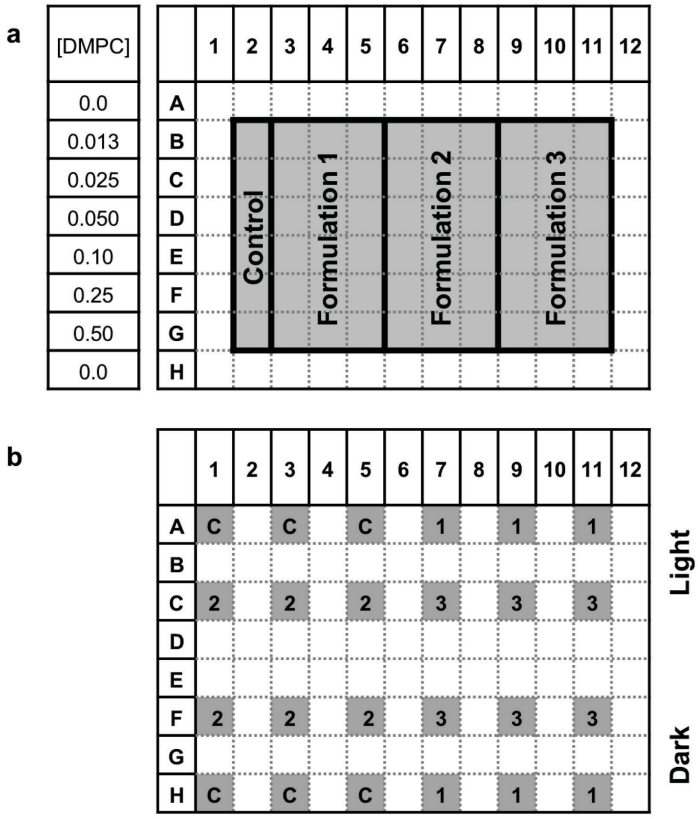

Figure 8.18. Plate design for photocytotoxicity assays. a) Plate design for an experiment using the inner 60 wells with a control column and three liposome formulations.[10] Each liposome formulation at each concentration is added to three different wells (technical triplicate). b) Plate design for an experiment using high intensity red light irradiation with three control wells (C) and three liposome formulations (indicated with 1, 2, and 3). The white wells have been left empty to avoid unintentional irradiation of neighboring wells. Only the top half of the wells was irradiated (12 wells in total).

Figure 8.19. Photographs of setup used for irradiation experiments with high intensity red light, consisting of a mini-incubator (1; for clarity here without 96-well plate), motorized XY-translation stage (2), and collimating lens fitted underneath the mini-incubator (3), connected to a fiber-coupled laser (not shown).

8.5 References

[1] a) R. E. Goldbach, I. Rodriguez-Garcia, J. H. van Lenthe, M. A. Siegler, S. Bonnet, *Chem. Eur. J.* **2011**, *17*, 9924-9929; b) B. S. Howerton, D. K. Heidary, E. C. Glazer, *J. Am. Chem. Soc.* **2012**, *134*, 8324-8327; c) L. M. Loftus, J. K. White, B. A. Albani, L. Kohler, J. J. Kodanko, R. P. Thummel, K. R. Dunbar, C. Turro, *Chem. Eur. J.* **2016**, *22*, 3704-3708; d) K. Arora, J. K. White, R. Sharma, S. Mazumder, P. D. Martin, H. B. Schlegel, C. Turro, J. J. Kodanko, *Inorg. Chem.* **2016**.

[2] a) M. Ferrari, *Nat. Rev. Cancer* **2005**, *5*, 161-171; b) Y. Matsumura, H. Maeda, *Cancer Res.* **1986**, *46*, 6387-6392.

[3] a) P. S. Wagenknecht, P. C. Ford, *Coord. Chem. Rev.* **2011**, *255*, 591-616; b) A. Bahreman, J.-A. Cuello-Garibo, S. Bonnet, *Dalton Trans.* **2014**, *43*, 4494-4505; c) S. L. H. Higgins, K. J. Brewer, *Angew. Chem., Int. Ed.* **2012**, *51*, 11420–11422.

[4] a) S. H. C. Askes, A. Bahreman, S. Bonnet, *Angew. Chem., Int. Ed.* **2014**, *53*, 1029-1033; b) S. H. C. Askes, M. Kloz, G. Bruylants, J. T. Kennis, S. Bonnet, *Phys. Chem. Chem. Phys.* **2015**, *17*, 27380-27390.

[5] A. Meister, M. E. Anderson, *Annu. Rev. Biochem.* **1983**, *52*, 711-760.

[6] M. Almgren, *J. Am. Chem. Soc.* **1980**, *102*, 7882-7887.

[7] a) H. J. Feldmann, M. Molls, P. Vaupel, *Strahlenther. Onkol.* **1999**, *175*, 1-9; b) P. Vaupel, F. Kallinowski, P. Okunieff, *Cancer Res.* **1989**, *49*, 6449-6465; c) E. E. Graves, M. Vilalta, I. K. Cecic, J. T. Erler, P. T. Tran, D. Felsher, L. Sayles, A. Sweet-Cordero, Q.-T. Le, A. J. Giaccia, *Clin. Cancer Res.* **2010**, *16*, 4843-4852.

[8] a) H.-J. Yang, C.-L. Hsu, J.-Y. Yang, W. Y. Yang, *PLoS One* **2012**, *7*, e32693; b) A. L. Magra, P. S. Mertz, J. S. Torday, C. Londos, *J. Lipid Res.* **2006**, *47*, 2367-2373; c) R. Chowdhury, M. A. Amin, K. Bhattacharyya, *J. Phys. Chem. B* **2015**, *119*, 10868-10875.

[9] S. A. Vinogradov, D. F. Wilson, *Journal of the Chemical Society, Perkin Transactions 2* **1995**, *0*, 103-111.

[10] S. L. H. Hopkins, B. Siewert, S. H. C. Askes, P. van Veldhuizen, R. Zwier, M. Heger, S. Bonnet, *Photochem. Photobiol. Sci.* **2016**, *15*, 644-653.

[11] a) Summary of Lipoplatin product characteristics, *http://lipoplatin.com/info_sop.php*, accessed on **13 July 2016**; b) Doxil prescribing information, *https://www.doxil.com/shared/product/doxil/doxil-prescribing-information.pdf*, accessed on **15 July 2016**

[12] a) T. M. Allen, A. Chonn, *FEBS Lett.* **1987**, *223*, 42-46; b) A. Gabizon, D. Papahadjopoulos, *Proceedings of the National Academy of Sciences* **1988**, *85*, 6949-6953; c) D. Liu, A. Mori, L. Huang, *Biochim. Biophys. Acta, Biomembr.* **1991**, *1066*, 159-165; d) A. L. Klibanov, K. Maruyama, V. P. Torchilin, L. Huang, *FEBS Lett.* **1990**, *268*, 235-237.

[13] Y. Sadzuka, K. Tokutomi, F. Iwasaki, I. Sugiyama, T. Hirano, H. Konno, N. Oku, T. Sonobe, *Cancer Letters* **2006**, *241*, 42-48.

[14] R. Weijer, M. Broekgaarden, M. Kos, R. van Vught, E. A. J. Rauws, E. Breukink, T. M. van Gulik, G. Storm, M. Heger, *Journal of Photochemistry and Photobiology C: Photochemistry Reviews* **2015**, *23*, 103-131.
[15] A. Bahreman, M. Rabe, A. Kros, G. Bruylants, S. Bonnet, *Chem. Eur. J.* **2014**, *20*, 7429-7438.
[16] S. Bonnet, B. Limburg, J. D. Meeldijk, R. J. M. Klein Gebbink, J. A. Killian, *J. Am. Chem. Soc.* **2010**, *133*, 252-261.
[17] S. L. H. Hopkins, B. Siewert, S. H. C. Askes, P. van Veldhuizen, R. Zwier, M. Heger, S. Bonnet, *Photochem. Photobiol. Sci.* **2016**.
[18] B. Siewert, V. H. S. van Rixel, E. J. van Rooden, S. L. Hopkins, M. J. B. Moester, F. Ariese, M. A. Siegler, S. Bonnet, *Chem. Eur. J.* **2016**, n/a-n/a.
[19] J. Reedijk, *Chem. Rev.* **1999**, *99*, 2499-2510.
[20] K. J. Takeuchi, M. S. Thompson, D. W. Pipes, T. J. Meyer, *Inorg. Chem.* **1984**, *23*, 1845-1851.
[21] A. Bahreman, B. Limburg, M. A. Siegler, E. Bouwman, S. Bonnet, *Inorg. Chem.* **2013**, *52*, 9456-9469.
[22] R. H. Zheng, H. C. Guo, H. J. Jiang, K. H. Xu, B. B. Liu, W. L. Sun, Z. Q. Shen, *Chin. Chem. Lett.* **2010**, *21*, 1270-1272.